### **Review Article**

Yuting Xie, Junyi Hu, Yuxin Hu, and Xiaosong Jiang\*

# A review on strengthening mechanisms of carbon quantum dots-reinforced Cu-matrix nanocomposites

https://doi.org/10.1515/ntrev-2024-0038 received July 15, 2023; accepted May 14, 2024

Abstract: Combination of metal matrix materials with carbon quantum dots (CQDs) can not only optimize the property of metal matrix materials, but also produce novel material systems with ultra-high performance or superior comprehensive performance. The excellent electrical, mechanical, and thermal characteristics of CQDs can compensate for some intrinsic defects of the metal matrices to improve the composite properties. The various interfaces formed through the different degrees of CQDs dispersion in the metal matrices are essential in the mechanism of the composite performance improvement. In this review, the research progress and results of CQDs in metal matrix composites are discussed and summarized, including the recent preparation methods of CQDs and carbon nanostructure-reinforced metal matrix materials, as well as the influences of the preparation methods on the material structures and properties. In addition, by focusing on the interfaces between CQDs and metal matrices in composite materials, the performance improvement and reinforcement mechanisms of the CQD-modified metal matrix composites are described from mechanical, electrical, and thermal aspects. Further studies on CQDs in metal matrix composites are still required to provide theoretical guidance for the preparation of CQDs-reinforced metal matrix composites with intensity and ductility above the average.

Nanotechnology Reviews 2024; 13: 20240038

### 1 Introduction

Carbon quantum dots (CQDs) are a kind of zero-dimensional nanoparticles (NPs) usually with quasi-spherical shape and diameters less than 10 nm. They comprise carbon, oxygen, and hydrogen elements, and typically have sp<sup>2</sup> hybrid conjugated nanocrystalline nuclei with a big amount of the oxygencontaining groups including carboxyl, hydroxyl, and carbonyl groups on the surface, which allow CQDs to be dissolved in water and some polar organic solvents [1-3]. As shown in Figure 1, CQDs have been broadly applied in various fields due to their unique structures and properties, such as upconversion fluorescence emission, excellent electron storage and transfer, convenient surface modification, designability of surface functional groups, as well as simple and diverse synthesis methods [4-7]. CQDs have different structures with amorphous and crystalline as the most common ones [8,9]. Through the combination or polymerization of CQDs and metal matrix materials, the mechanical, friction, electrical, and thermal performances of metal matrix materials can be optimized. To continuously develop more advanced composite materials, extensive studies have been conducted from different aspects.

Some drawbacks of traditional carbon nanomaterials, such as poor mechanical properties and easy aggregation, greatly limit their widespread application in various fields. To address these problems, a large amount of research work have been carried out worldwide. Niyogi *et al.* [10] successfully improved the mechanical property of microjet carbon nanomaterials by using ultrasound to break the van der Waals force between the molecules in the material and reduce their surface energy. Rashad *et al.* [11] prepared fine powder of carbon/metal matrix composite with good performance by mechanically dispersing carbon nanomaterials through the mutual collision and shear force between

Yuting Xie, Yuxin Hu: School of Physical Science and Engineering, Beijing Jiaotong University, Beijing, 100044, China; Department of Chemistry, Waterloo Institute for Nanotechnology, University of Waterloo, 200 University Avenue West, Waterloo, ON, N2L 3G1, Canada Junyi Hu: SDU-ANU Joint Science College, Shandong University Weihai, Weihai, Shandong, 264200, China

**Keywords:** carbon quantum dots, metal matrix composites, material properties, preparation methods, strengthening mechanisms

<sup>\*</sup> Corresponding author: Xiaosong Jiang, School of Materials Science and Engineering, Southwest Jiaotong University, Chengdu, Sichuan, 610031, China, e-mail: xsjiang@swjtu.edu.cn, tel: +86-28-87634177; fax: +86-28-87634177

2 — Yuting Xie et al. DE GRUYTER

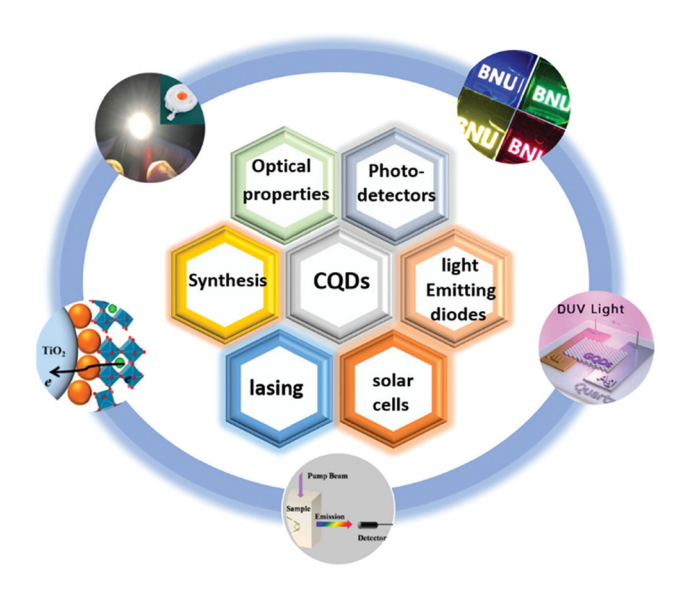


**Figure 1:** The recent applications of CQDs in the field of optoelectronics [4–7,19–21].

the steel ball and the powder in the presence of alcohol and other solvents to protect the structure of the material from being damaged. Nam et al. [12] adopted a surface modification procedure, including acidification, nitration, and surface chemical reaction, to modify the surface properties (such as water solubility) of carbon nanomaterials. By this means, the compatibility of the material was improved. Aiming at solving the poor wettability problem between carbon and copper in the matrix composite, Chu et al. [13] introduced new elements and Cr particles into the system, which caused the formation of Cr<sub>7</sub>C<sub>3</sub> NPs and Cu-Cr interfaces in the carbon nanomaterials/copper matrix, improving the interface bonding strength. With the continuous intensive research on carbon nanomaterials-reinforced metal matrix composites, many new preparation methods have been proposed, and various new types of carbon nanomaterials have been developed, which show high resistance to particle agglomeration, easy dispersion, and good wettability with metal matrices.

Although CQDs could ameliorate the mechanical performances of metal matrix composites to some extent, the research achievements often fail to meet the targets of experimental design. This is mainly because CQDs have strong agglomeration tendency under the van der Waals force [14], resulting in irreversible negative effects on the electrical, mechanical, and thermal performances of metal matrix composites. Song *et al.* used an one-step "bottom-up" strategy for *in situ* preparation of carboxylated CQDs at ambient temperature, which were then applied to induce the synthesis of 2D NiFe-MOF-NSs by expanding the NiFe-MOF layer spacing, increasing the positive charges of the

active sites, and improving the oxygen evolution reaction (OER) property of NiFe-MOF [15]. However, to achieve practical applications of CQDs in electrical and thermal fields, many issues still need to be overcome. For example, because of the low wettability between carbon and metal matrix [16,17], it has high difficulty to form an effective bonding interface between CQDs and metal matrix composites, which restricts the performances of metal matrix composites. Li et al. investigated the interfacial binding effect between CQDs and Ru, where they identified a synergistic effect. The powerful coordination interaction between the Ru d orbitals and functional groups on the COD surface successfully immobilized Ru NPs and prevented them from aggregation, facilitating the formation of the binding interface between Ru NPs and CQD. In addition, many CQD modification techniques have been used to ameliorate the CQD dispersion in composites and to strengthen the interface bonding ability. However, these methods are not able to completely eliminate the phenomenon of CQDs agglomeration, and there are still unavoidable problems in practical applications [15.18]. Therefore, further studies on the relevant topics are still highly desired to ameliorate the comprehensive performance of CQDs-modified metal matrix composites, and special focuses should be placed on inhibiting NP agglomeration, increasing wettability between carbon and metal matrix, improving interface bonding ability, and enhancing mechanical performance of composite materials.

Modification of the metal matrix composite with CQDs could greatly improve the mechanical, friction, electrical, and thermal performances of the material. However, currently there are still some problems in the practicability of the composites, and thereby a series of studies on these issues have been conducted worldwide. It is necessary to summarize the research progress of CQDs-modified metal matrix composites to clarify the performance characteristics of the composite materials. This will contribute to the theoretical guidance for design and preparation of metal matrix composites with superior performances, such as excellent conductivity and heat transfer efficiency, strong tensile properties, and high hardness, which can accelerate the practical application of the metal matrix composites in aerospace, microelectronics, optics, and new energy fields.

In this study, the research efforts for improving the comprehensive performances of CQDs-modified metal matrix composites are systematically reviewed from mechanical, electrical, and thermal aspects. First, several typical preparation methods of CQDs and their reinforced metal matrices are introduced. These preparation processes have critical impacts on the various performances of the composite materials. Second, the influences of CQDs on the interface of metal

matrix composites are evaluated and summarized. The application and mechanism of the CQDs/metal interface in composites for improving mechanical properties, reducing electron and phonon scattering are emphatically described. Besides, the enhancement mechanism of the CQDs reinforcement phase is analyzed. Finally, the developments of functional and structural integrated high-performance metal matrix composites are discussed and prospected from the points of view of numerical simulation, AI, and machine learning (ML). Until now there are only very few publications about numerical simulation, AI, and ML in CQDs-reinforced metal matrix composites. Therefore, this topic is not specifically discussed in this study; however, it is a research hotspot for the future.

### 2 Preparation method of CQDsreinforced metal matrix composites

### 2.1 Preparation method of CQDs

There are many ways to prepare CQDs, among which the two most commonly employed ones are the "top-down" and "bottom-up" methods using carbon materials and organic molecules as carbon source, respectively. "Top-down" refers to cutting or splitting large blocks of materials with carbon structure, *e.g.*, nano diamonds, carbon nanotubes, graphene, carbon black, graphite oxide, and activated carbon, into small particles of CQDs through arc discharge, electrochemical oxidation, laser ablation, *etc.* "Bottom-up" is to obtain CQDs from precursors containing carbon atoms, such as citric acid, sugar,

polymer-silica nanocomposite, *etc.*, through combustion/heat treatment-assisted synthesis or microwave synthesis. The selected synthesis method and carbon source material usually determine the physical and chemical performances of the as-prepared CQDs, including fluorescence characteristics, quantum yield, biocompatibility, water dispersibility, and oxygen/nitrogen content. Figure 2 lists several typical preparation methods of CQDs [22].

### 2.1.1 Top-down method

The top-down method uses chemical or physical methods to cut large carbon materials (graphite, carbon fiber, fullerene, graphene oxide (GO), *etc.*) at nanometer scale to prepare small size CQDs. As shown in Table 1 and Figure 3, laser ablation method [23], electrochemical method [24,25], chemical oxidation method [26], and arc discharge method [27] belong to the top-down methods. The CQDs prepared by top-down procedure have advantages of abundant raw material, simple production method, and cheap price. Therefore, they can be made in huge scales. However, this method has not achieved great success in synthesizing CQDs with uniform diameters and well-controlled particle sizes.

### 2.1.1.1 Strong acid oxidation method

Strong acid oxidation method is one of the most widely used methods for preparation of CQDs by utilizing strong acid to chemically peel off carbon sources. This method can generate more edge defects and is capable for the mass production of CQDs. Although the acid oxidation stripping method has the advantages of easy access to raw materials,

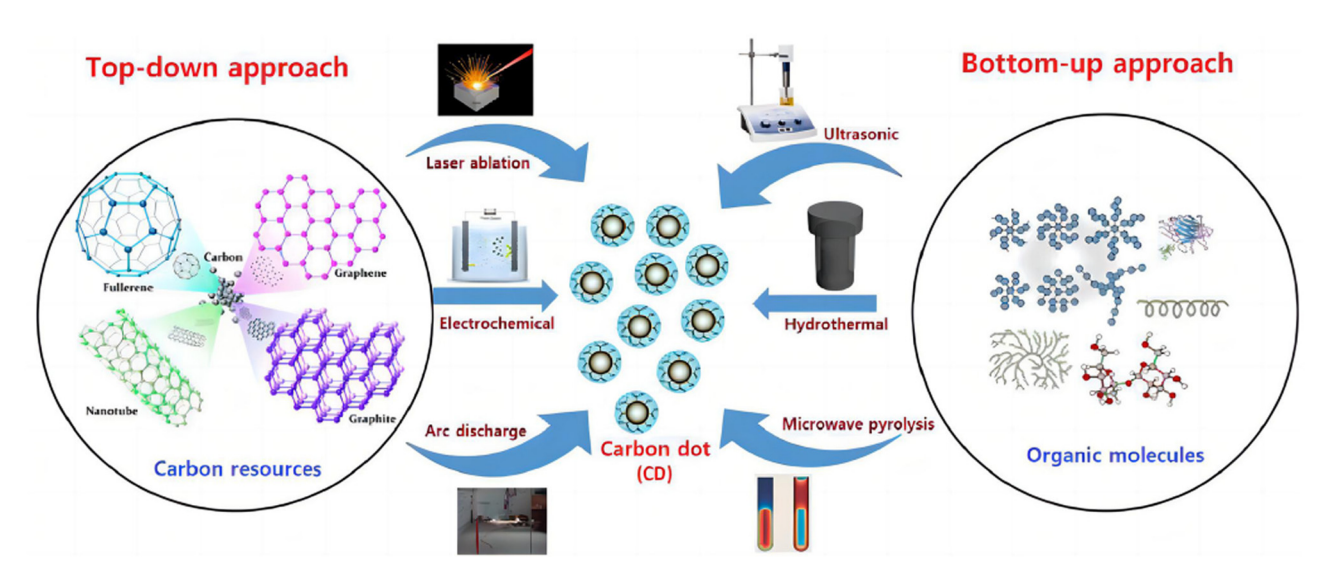
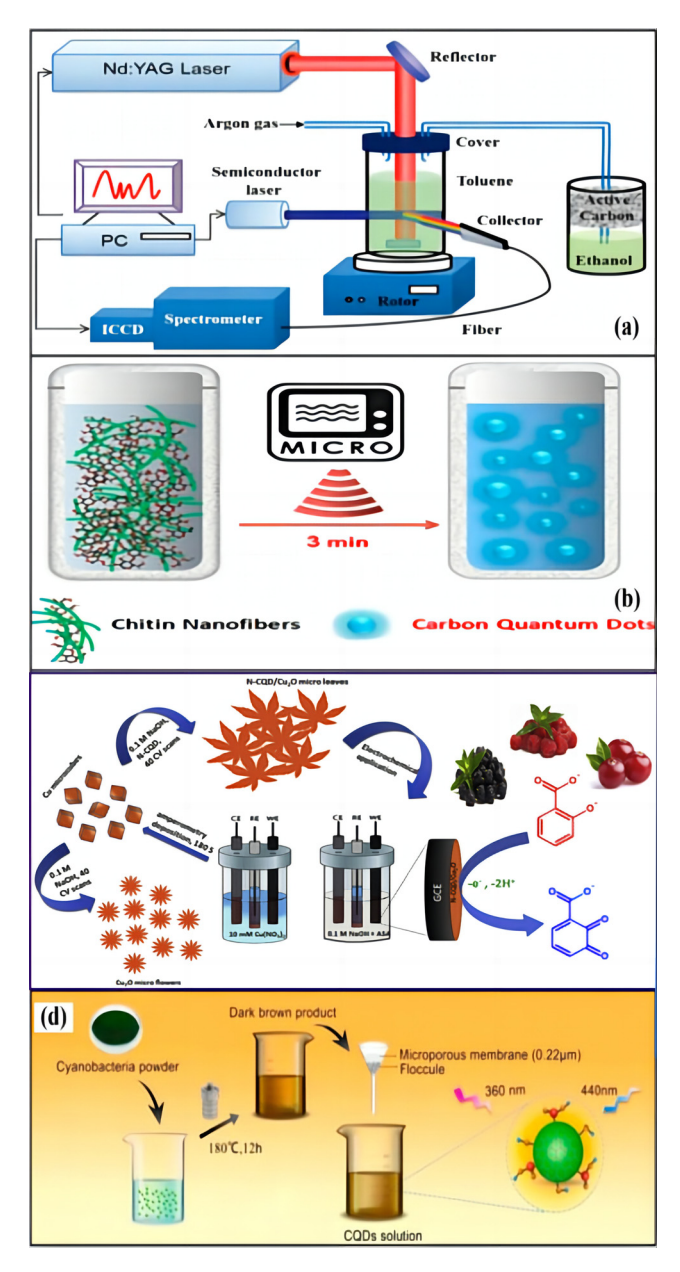


Figure 2: Schematic illustration of the preparation method of CQDs [22].

Table 1: Example of recent CQDs and their preparation method

Methods	Comprehensive approach	Source	Quantum yield (%)	Size range (nm)	Application/properties	Ref.
Top-down method Laser ablation Laser ablation Laser ablation	Laser ablation Laser ablation Laser ablation	30 nm thick films of amorphous carbon Carbon fiber cloth Empty fruit bunch	ND 35.4 —	20–300 ~100 21.46, 19.96, and 16.07	Sensors PL emission mechanism and cell bioimaging Detection of sugar	[23] [28] [29]
	Non-focusing pulsed laser irradiation Toluene Electrochemical electrolysis Ethanol Chronoamperometric method 1-Propar Two-step oxidation Anthraci High-temperature acid oxidation Multi-wa	Toluene Ethanol 1-Propanol Anthracite Multi-walled carbon nanotubes	18 9.5, 11.2, and 4.6 — 18.9, 12.6, and 4.3	3-4 Less than 10 5-10	PL Detectionof Fe <sup>3+</sup> , Cell imaging and cytotoxicity measurement Determination of dopamine (DA) and epinephrine PL	[30] [31] [32] [26]
Bottom-up method	Pyrolysis Pyrolysis Pyrolysis Microwave-assisted Microwave-assisted Microwave-assisted Hydrothermal Hydrothermal Hydrothermal	Chia seeds Finger millet ragi Urea, citric acid, and polyethyleneimine ND Roasted Chickpeas Fresh lemon juice SCG (Arabica) Banana peel waste Cambuci juice (Campomanesia phaea) Lemon juice Citric acid Rosehip fruit	ND ND 26 1.8 31 4.25 5 21.3 79 7.2, 9.6, and 23.8	4 6 1.91 and 1.61 ~10 4.5-10.3 1-6 2-40 4-6 3.7 4.5 5.5-3	Electrochemical sensors Biosensor Photocatalytic degradation of rhodamine B Sensing of Hg <sup>2+</sup> Sensing of Fe <sup>3+</sup> Good selectivity for Hg <sup>2+</sup> Antimicrobial Bioimaging Sensing of Zn <sup>2+</sup> Biosensors Waste water treatment Bioengineering applications	[34] [35] [36] [37] [38] [40] [41] [42] [43]



**Figure 3:** Synthesis approaches of CQDs: (a) laser ablation method [30], (b) microwave method [51], (c) electrochemical method [52], and (d) oxidation method [53].

low cost, and high yield, it also shows problems such as harsh reaction condition, time-consuming process, and complex post-treatment. Besides, the use of acidic oxidants cannot meet the green preparation requirement due to the induced environmental problems.

As shown in Figure 4, Kushwaha *et al.* [33] synthesized CQDs through the application of strong acid oxidation. This process involved the oxidation of MWCNTs at 350°C using concentrated  $\rm H_2SO_4$  and  $\rm HNO_3$ , resulting in CQDs with diameters ranging from 5 to 10 nm. The synthesized CQDs were characterized by a significant presence of oxygen-containing

functional groups on their surface, imparting excellent water solubility. Besides, it was found that the photoluminescence (PL) peak of CQDs synthesized by strong acid oxidation is independent of the excitation wavelength in the visible light range. Boruah et al. [46] synthesized CQDs by using waste biomass bagasse and taro scalp as the precursors and H<sub>2</sub>O<sub>2</sub> as the oxidant, in which the CQDs synthesized with taro scalp showed the highest fluorescence quantum yield (26.2%). Hu et al. [47] documented a new type of nitrogen (N)-doped CQDs prepared by strong acid oxidation of coal tar pitch at medium and low temperatures, which exhibited a quantum yield of around 7.0%. This method could improve the water solubility and the fluorescence characteristic of the as-prepared CQDs, but it has high requirements for the reaction conditions. Therefore, the strong acid oxidation method for CQDs preparation is considered as a non-environmentally friendly process due to its harsh reaction conditions and complex post-treatment procedures.

### 2.1.1.2 Electrolysis

Electrolysis conventionally employs carbon-based materials both as the working electrode and as the carbon precursor. Upon application of a voltage across the electrodes, an oxidation reaction occurs at the anode, facilitating the detachment of carbon material from the electrode surface. This phenomenon results in the generation of CQDs. Graphite rods, MWCNTs, graphite powder, carbon fibers, and so on can be utilized as the carbon electrode material [48]. Sodium hydroxide, phosphate buffer solution, tetrabutylammonium perchlorate, potassium persulfate and ultra-pure water can be used as electrolyte solutions [49]. In addition, the electrolyte could also be used as the carbon source to realize the bottom-up electrochemical synthesis of CQDs. This electrochemical method shows advantages of easy access to equipment, simple operation, and high purity of the CQDs products (Figure 5). Therefore, it is more widely used than the other methods [32]. However, up to now, electrochemical methods have succeeded only in synthesis of CQDs emitting blue, green, and yellow fluorescence, and not in preparation of CQDs with longer wavelength emission.

In 2016, Liu *et al.* [31] prepared CQDs with high crystallinity and average diameter of around 4.0 nm in NaOHcontaining ethanol solution by using a simple electrolysis process with a graphite working electrode and a constant potential for 3 h. The formed CQDs show a gradual color change from colorless to bright yellow with the increase in the temperature from 4°C to the ambient temperature. Moreover, the influence of the applied voltages on the preparation of CQDs was also investigated. The results

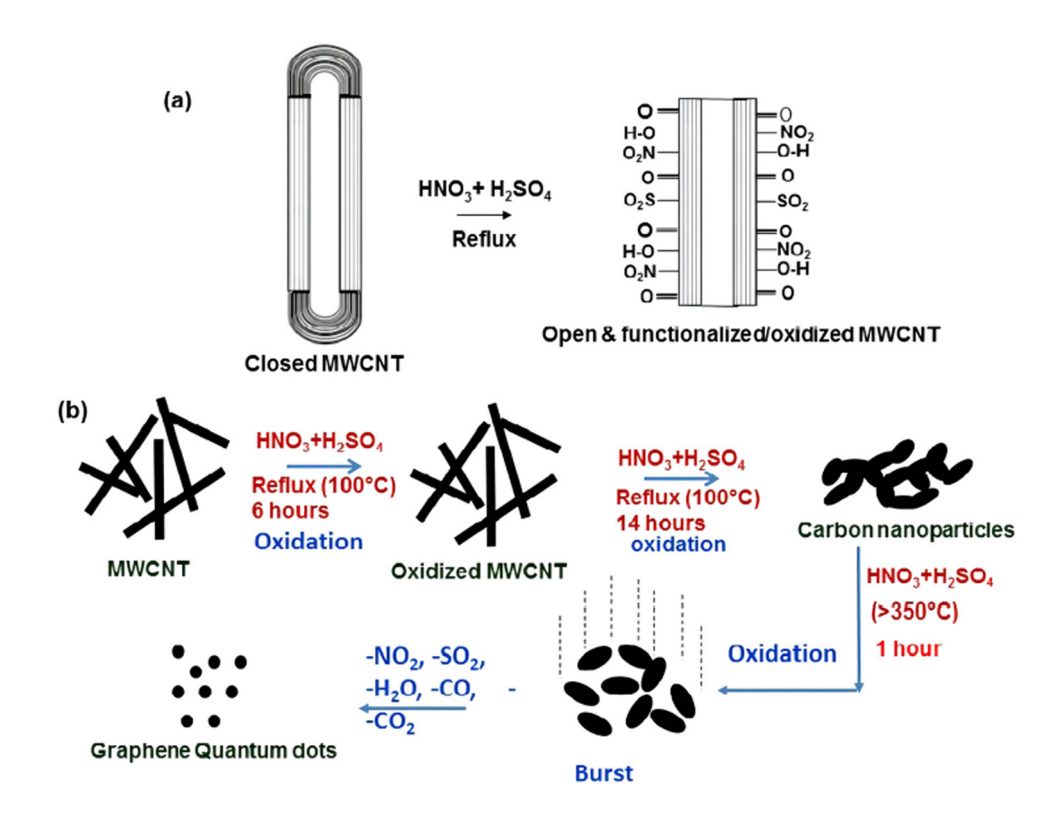


**Figure 4:** Proposed mechanism for the generation of CQDs via high-temperature acidic oxidation of multiwalled carbon nanotubes (MWCNTs). (a) The graphene layer on the surface wall of carbon nanotubes is oxidized by acid reagents, resulting in the formation of carbonyl, carboxylic, sulphur oxide and nitro groups on MWCNTs' surface. (b) The increase in reaction time causes oxidation of the graphene layers underneath the surface wall, resulting in nanotubes bending, buckling, and folding [33].

indicate that higher voltage leads to the formation of CQDs with larger sizes. Shinde and Pillai [50] used CNTs as the precursor to synthesize CQDs with electrochemical method in propylene carbonate solution containing high concentration

of lithium chlorate. This method is simple in operation and the obtained CQDs are uniform in particle size; however, a very low yield of 6.1% could only be achieved with this method. Tian *et al.* [54] documented the fabrication of CQDs

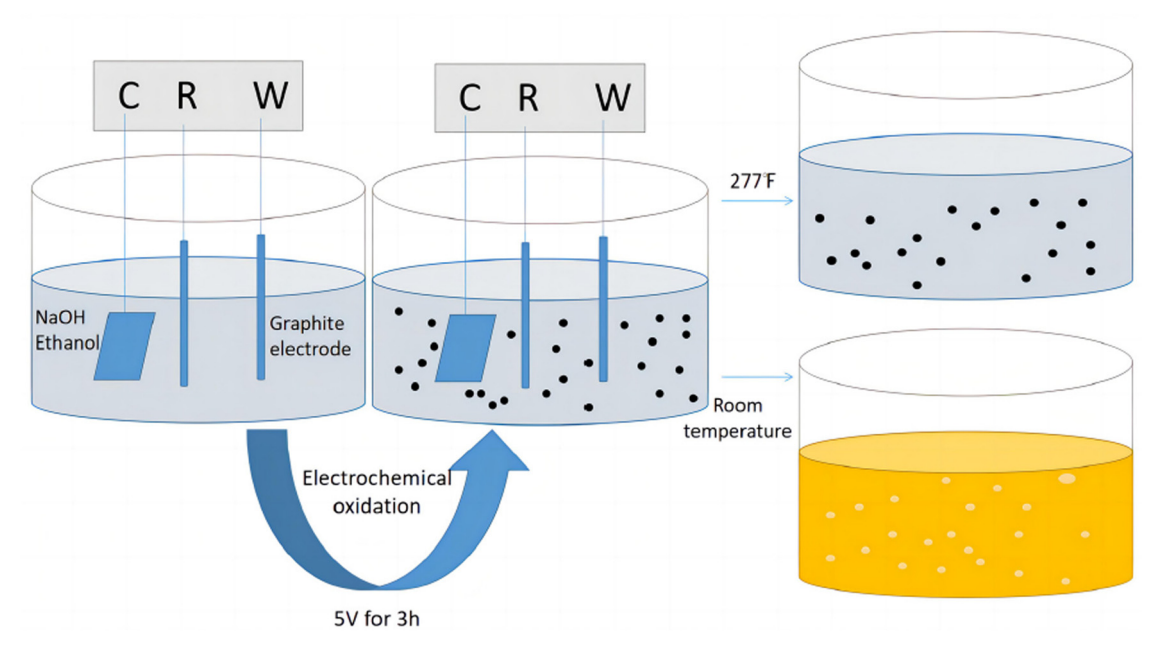


Figure 5: Schematic diagram of CQDs formation through electrochemical oxidation on graphite electrode.

employing an electrolytic strategy, wherein inorganic salts served as the electrolytes, and graphite rods were utilized as electrodes for both the anode and cathode. They investigated the impact of various electrolyte solutions on the properties of the synthesized CODs. Their findings revealed that CQDs synthesized using a nitrate-based electrolyte exhibited desirable morphological characteristics and possessed an average diameter of 3.15 nm. Generally, electrochemical methods use conductive carbon materials such as graphite rods, graphene, graphite paper, etc., as the working electrode. By applying a voltage, the electrode is subjected to anodic oxidation and ions from the electrolyte enter the graphite layer. The large carbon materials are peeled off into small carbon NPs, and the mixed solution obtained by electrolysis is subsequently centrifuged to collect a suspension of CQDs. After dialysis purification treatment, a pure solution of the target product could be finally obtained. This electrochemical preparation has good reproducibility and the as-prepared CQD products show high stability. In sum, the electrochemical methods have no requirements for harsh reaction conditions. They are simple and green process for CQDs preparation.

#### 2.1.1.3 Laser ablation method

Laser beam with high energy is usually used in laser ablation method for bombarding the carbon targets to peel off the carbon nanosized particles, which are subsequently passivated into CQDs. It is worthy to note that the employment of suitable carbon target materials or media in the laser ablation technique enables the direct generation of CQDs without necessitating an additional passivation step. In addition, the morphology of CQDs can be controlled with the pulse width, energy density, and wavelength of the laser beam. As one of the earliest approaches for CQDs preparation, laser ablation has the advantage of operation simplicity and the disadvantages of undesirable CQDs wave length, expensive equipment, time-consuming process, and so on, restricting its wide application.

Sun et al. [55] first synthesized CQDs using laser ablation method in 2006. Under water vapor atmosphere, carbon NPs without fluorescence effect were prepared by laser etching of mixed carbon targets of the graphite powder and cement at 900°C and 75 kPa using argon as the carrier gas. Afterwards, the system was refluxed in nitric acid aqueous solution, passivated with polyethylene glycol (PEG) 1500 (PEG1500N), and finally treated with acid to obtain different CQDs (Figure 6) with quantum yield of 4-10%. Li et al. [56] dissolved carbon nanomaterials in organic reagents and used laser to prepare and passivate CQDs in one step, simplifying the operation process of laser etching method. In addition, by adjusting the organic solvent, CQDs can be passivated by different agents. Recently, Cui et al. [28] synthesized blue fluorescent CQDs with low-cost carbon fiber cloth by using a self-made double-beam pulsed laser ablation system. In the preparation process, the laser beam was divided into two through a beam splitter to improve the ablation rate and shorten the preparation time. Compared to the products of single pulse laser ablation, the CQDs prepared by this double-beam method have more uniform size, higher quantum yield of up to 35.4%, and good anti-interference performance, which can be used for HeLa cell imaging research. The instruments required for laser ablation preparation of CQDs are relatively expensive, and the surface of the as-prepared CQDs usually needs to be modified with organic solvents to produce fluorescence. Due to the addition of organic reagents, the subsequent purification process of CQDs becomes relatively complicated.

In summary, the top-down methods are to peel and cut bulk carbon black, graphite, graphene, or other carbon materials into nanosized CQDs through laser ablation, arc discharge, acid oxidation, thermal decomposition, and electrochemical processes. The carbon sources usually contain graphite microcrystals or a large number of sp<sup>2</sup> conjugated microregions. The top-down preparation methods show advantages of high yield, easy functionalization, and simple operation, but they also have the disadvantage of the high difficulty in CQDs size and morphology control.



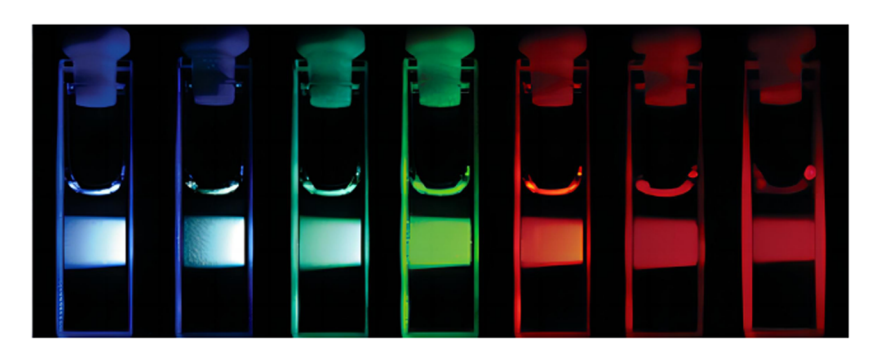


Figure 6: PEG1500N CQDs after passivation [55].

#### 2.1.2 Bottom-up method

The bottom-up method is to carbonize organic molecular precursors (*e.g.*, citric acid, ascorbic acid, ethylene glycol, phenylenediamine, *etc.*) through heat treatment to prepare CQDs. As shown in Table 1, pyrolysis [57], microwave-assisted synthesis [37–40], and hydrothermal/solvothermal synthesis [58] belong to bottom-up methods. The bottom-up methods can effectively control the composition, size, morphology and other characteristics of CQDs by using different precursors and carbonization conditions. Besides, they could also improve the quantum yield of CQDs. However, these methods usually require complex multiple synthesis steps and time-consuming subsequent purification processes.

### 2.1.2.1 Pyrolytic method

The pyrolysis approach usually comprises the following steps: The carbon source is carbonized at high temperature, and the CQDs are obtained after filtration, centrifugation, dialysis, chromatographic separation, and other post-treatment purification. In addition, different surface passivators and precursors can be used to control the hydrophilicity/hydrophobicity and atomic doping type of CQDs. There are some advantages in the preparation of CQDs by pyrolysis, like simple operation, low cost of carbon source, and large-scale preparation. However, this method is time- and energy-consuming, and it contains tedious post-pyrolytic treatment and purification processes. In addition, pyrolysis is not capable for preparation of long-wavelength CQDs, which restricts the application of pyrolytic CQDs in the biomedical field.

Xue *et al.* [59] reported the pyrolysis of organic precursor peanut shells to prepare fluorescent CQDs with low cytotoxicity, which can be used for multi-color imaging of living cells. By using a solid-state pyrolysis process with citric acid as the carbon source, Soumen et al. [60] synthesized CQDs with high water solubility, strong photostability, and excellent dispersibility. This method can directly cleave the carbon material in the absence of any solvents, simplifying the preparation steps. As shown in Figure 7, Supchocksoonthorn et al. [61] synthesized blue light CQDs using maleic anhydride (MA) as raw material through one-pot thermal decomposition. The typical synthesis process was reported as follows: 30 mL of MA solution (1.36 mol/L) was added into a crucible containing 20 mL of HNO<sub>3</sub> (2.5 mol/L), and then pyrolysis was conducted at 250°C for 4 h. After purification, a light-yellow solid was obtained with a yield of 54%. The synthesized CQDs show good selectivity for pyrimidine in bactericide- and metal ion-containing medium, and could be successfully used for the detection of pyrimidine in food and drinking water with a recovery rate of 98.6-107.1%. The CQDs prepared by pyrolysis method has even size, and their surfaces are usually functionalized with various organic groups, including amino, carboxyl, and hydroxyl groups, which make the CQDs soluble in water.

### 2.1.2.2 Microwave-assisted synthesis

The microwave-assisted preparation method uses the radiation microwave as the heat source to provide energy for the reaction. After absorbing the microwaves, the reactants convert the electromagnetic radiation into internal energy, thus initiating the synthesis process. Microwave heating is uniform and fast, which shortens the reaction time and improves the yield of CQDs. Compared to other CQDs preparation approaches, the microwave method is more convenient and time-saving; therefore, it has the potential of industrialization for large-scale production of CQDs. However, a disadvantage of this method is the inhomogeneous particle size of the resulted CQDs. Besides, the particles with larger sizes cannot be separated by dialysis alone.

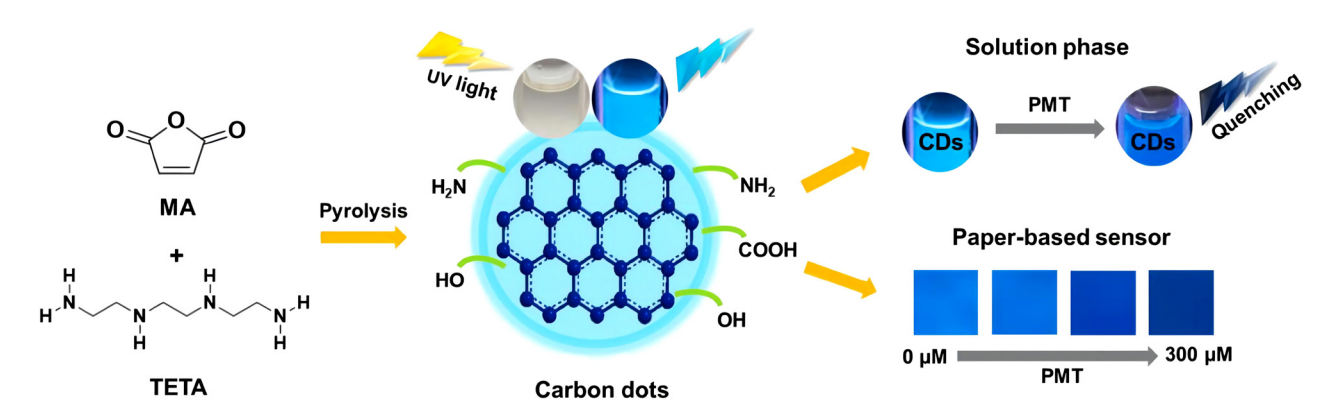


Figure 7: Preparation of CQDs by pyrolysis of MA and triethylenetetramine for detection of pyrimethanil [61].

Zhu et al. [62] heat treated different amounts of PEG and sugar solutions with a microwave oven until the solution transitioned from yellow to dark brown, resulting in well-dispersed CQDs with high fluorescence intensity. By utilizing flour as the carbon source, Oin et al. [63] prepared CQDs with a particle size of 1-4 nm, demonstrating their applicability in the detection of Hg<sup>2+</sup>. Wei et al. [64] synthesized CODs in a microwave-assisted guick reaction process with glucose as the carbon precursor and PEG-200 for surface passivation. In this specific process, 20 mL of PEG-200 was added to the mixture of 4 g glucose and 6 mL of ultrapure water. Afterwards, the mixed system was heat treated in a microwave reactor for 3 min, yielding CQDs. The resulting CQDs exhibited good conductivity, and they can be used to selectively detect ascorbic acid after electro-polymerization on the glassy carbon electrode (GCE). Besides, Zhang et al. [65] synthesized CQDs with glucose precursor using the microwave method under 150°C and 500 W of microwave power for 7-11 min (Figure 8), and Architha and Shobana [66] successfully prepared the blue fluorescent CQDs with a maximum quantum yield of 17% through microwave assisted reflux method with peppermint as the precursor (Figure 8).

### 2.1.2.3 Hydrothermal/solvothermal method

Hydrothermal/solvothermal method is to disperse small molecular reactants into water or other organic solvents, and then polymerize and carbonize them at elevated temperature and pressure in closed system to produce CQDs. The solvothermal process, an evolution of the hydrothermal method, distinguishes itself by employing organic solvents

instead of water. The hydrothermal or solvothermal method has gained widespread adoption for synthesizing CQDs owing to its straightforward operation, cost-effectiveness of the required apparatus, convenient subsequent processing, and wide range of carbon sources (such as the cheap and readymade carbon materials of banana peels, hair fibers, grass, and leaves) (Figure 9).

Lu et al. [67] prepared nitrogen-doped CQDs (N-CQDs) with 1,2,4-triaminobenzene (TAB) as the carbon source using the solvothermal approach. In this synthesis process, 100 mg 1,2,4-TAB precursor was first added to 10 mL of formamide. The system was subsequently heated to 120°C and sustained for 12 h, and through centrifugation large particles were removed. Afterwards, purification of the obtained solution was conducted using column chromatography with silica gel adsorbents and mixed dichloromethane and methanol (volume ratio of 2:8) as eluent. Finally, the as-resulted mixture was concentrated with a rotary evaporator to collect the purified product N-CQDs. The obtained yellow-green fluorescent N-CQDs have a quantum yield of 5.11% and high photostability. They can be applied to detect trace amount of Ag<sup>+</sup> in the food packaging materials.

Xu et al. [68] utilized citric acid as a precursor in the hydrothermal synthesis of CQDs, and then prepared metal matrix composites CDs@MOF-253. The carbon dots (CDs) synthesized by this method show good morphology and structure with uniform particle size of 1–5 nm, and without obvious particle aggregation. The Transmission Electron Microscopy (TEM) images (Figure 10) show that most of the CDs are amorphous carbon particles. This is further confirmed by the wide peak around 25° (0.34 nm) in the

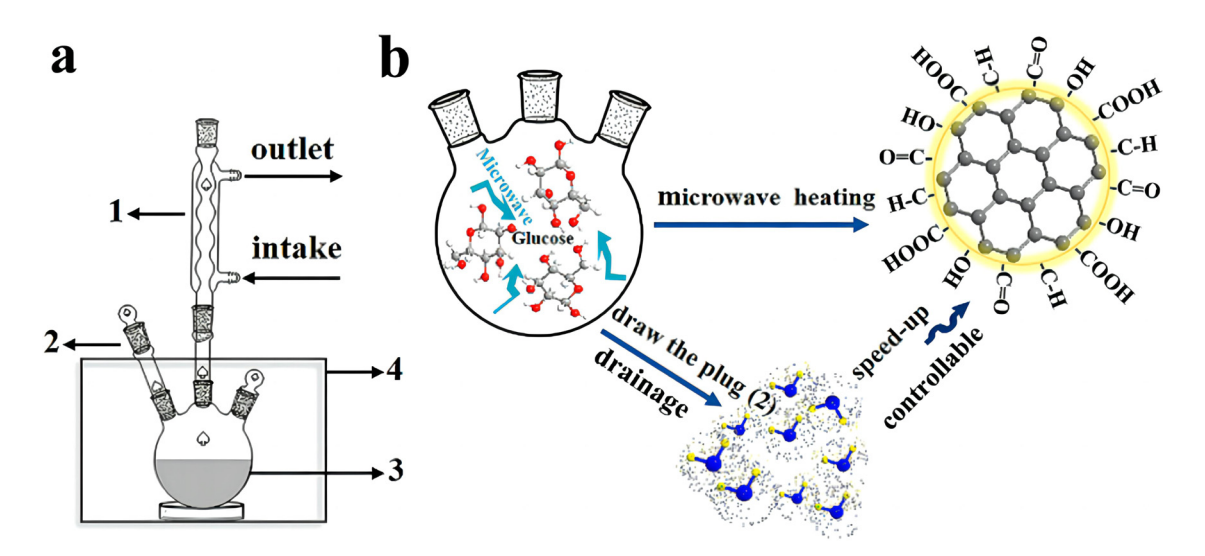


**Figure 8:** (a) A schematic of the experiment installing (1) the coolant system, (2) the drainage control system, (3) the reaction solution, and (4) the microwave work box. (b) A schematic illustration of the synthesis process of CQDs [65].



Figure 9: Synthesis procedure of CQD derived from Mexican mint [66].

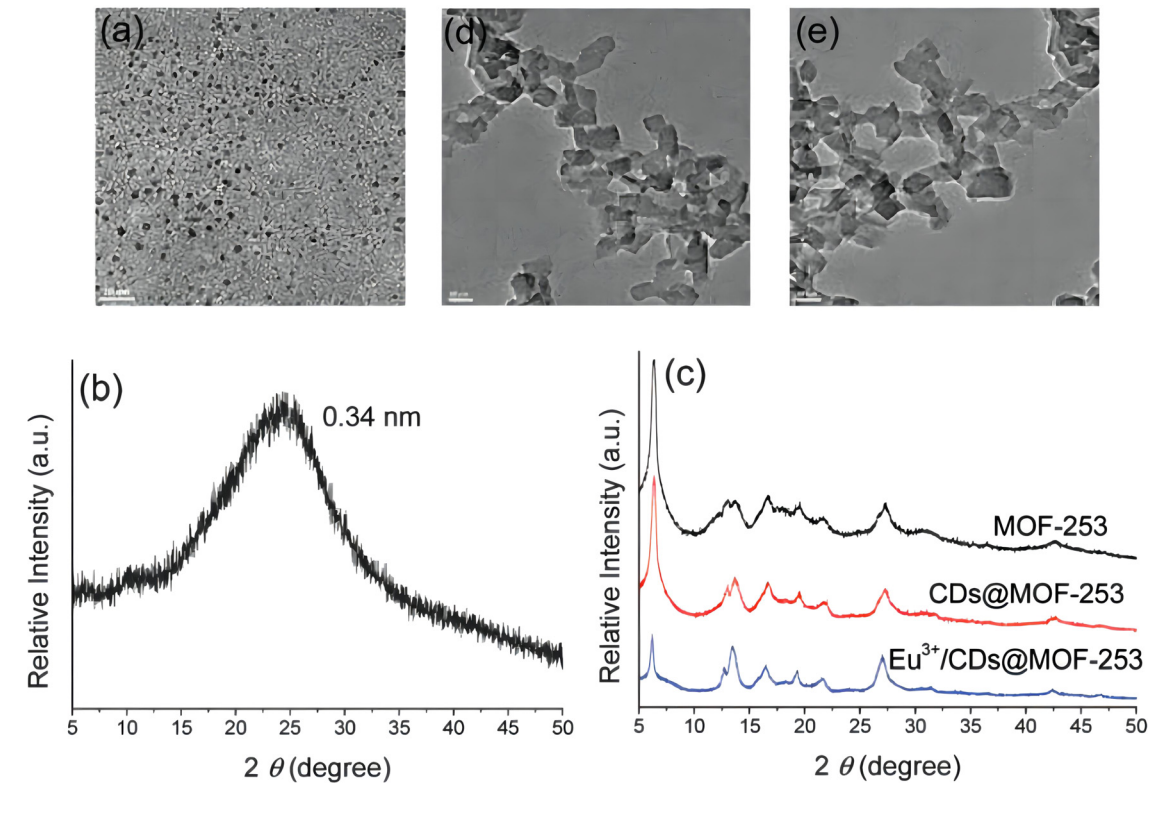


**Figure 10:** (a) TEM image with 10 nm scale bar, (b) XRD pattern of as-synthesized CQDs, (c) XRD patterns of MOF-253, CDs@MOF-253, and Eu3+/CDs@MOF-253, (d) TEM image of CDs@MOF-253 with a 50 nm scale bar, and (e) TEM image of Eu3+/CDs@MOF-253 [68].

X-ray diffraction (XRD) pattern of CDs. The CDs@MOF-253 composite material was synthesized by hydrothermal treatment of a mixture containing the CQDs and metal-organic framework (MOF) precursors. The results of XRD and TEM measurements show that the MOF framework and nanoplate morphology maintain their integrity after the reinforcement of the metal matrix material with CDs.

In addition, Bourlinos *et al.* [69] used the hydrothermal method to treat ammonium citrate at 300°C and obtained soluble and fluorescent CQDs. As shown in Figure 11, Xu *et al.* [70] prepared water-soluble CQDs with strong blue fluorescence using this method and potatoes as the organic precursor. The results suggest that CQDs prepared by hydrothermal method usually have good water solubility.

Until now, many hydrothermal methods for preparation of CQDs have been developed, mainly due to their low preparation cost and easy access to a variety of carbon sources. In addition, compared to other preparation methods, the hydrothermal process is more environmental friendly. The disadvantage of the hydrothermal method is the low efficiency of CQDs production.

### 2.2 Preparation of CQDs-reinforced metal matrix composites

This review focuses on the reinforcement of metal matrix with CQDs, and the studies on the use of CNTs within metal matrix composites are not included. However, similar to the case of CQDs, it is crucial to achieve an even dispersion of the carbon nanomaterial in the CNTs-reinforced metal matrix systems [71]. CNTs also have a tendency for agglomeration, which negatively affects the properties of the composites. Therefore, the methodologies developed for suppression of CQDs from agglomeration can also provide insights into the preparation of metal matrix composites-reinforced with uniformly dispersed CNTs [72,73]. By optimizing the techniques for preparation of CQDs and control of their dispersion in the metal matrices, the unique properties of CQDs can be leveraged to improve the mechanical, electrical, and thermal performances of the resulting composites.

When combining CQDs with metal matrix materials, the CQDs are very easy to agglomerate due to their poor dispersion in the system, resulting in irreversible negative

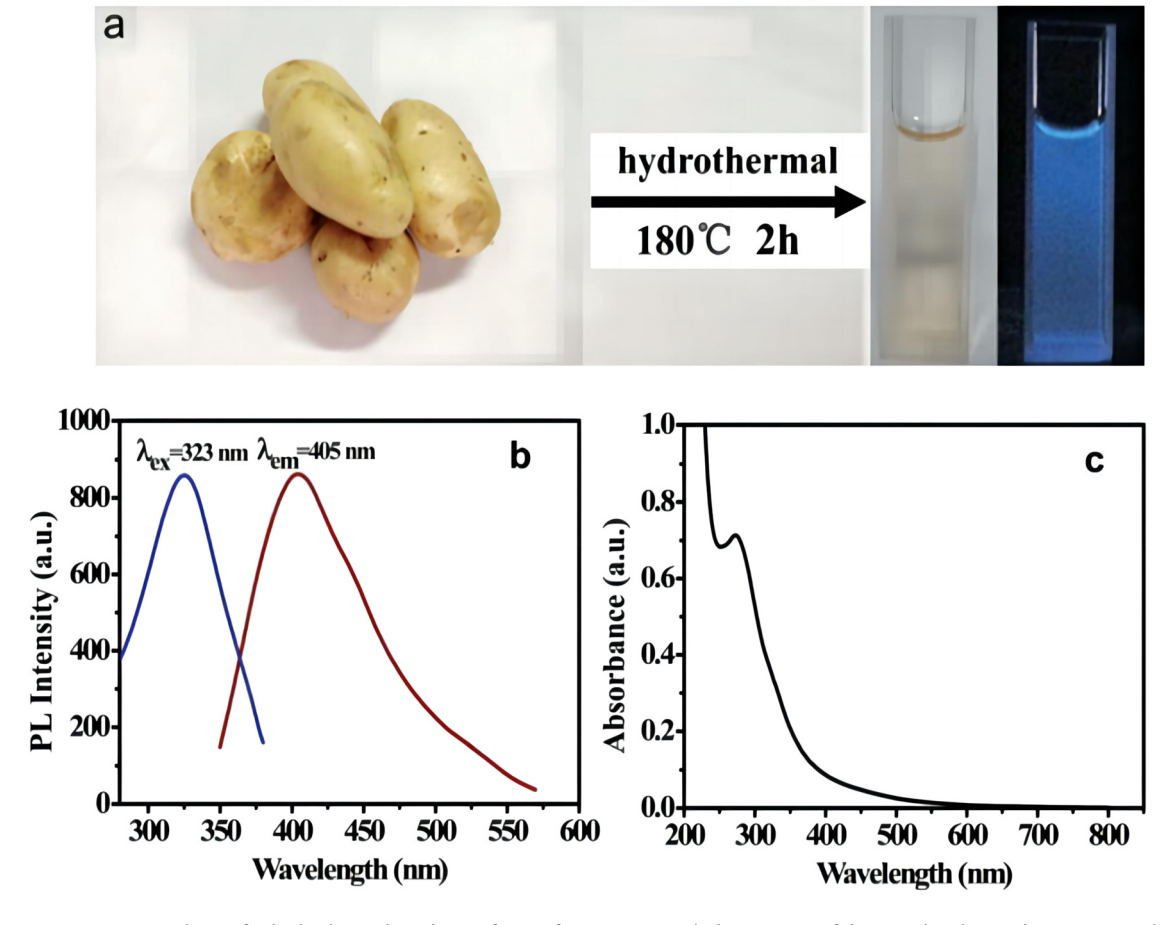


**Figure 11:** (a) Reaction conditions for hydrothermal synthesis of CQDs from potato (including images of the sample taken with a 365 nm UV laser and in natural light), (b) PL excitation and emission spectra, and (c) the CQDs' UV-Vis absorption spectrum [70].

effects on the as-prepared metal matrix composites, and reducing the performances of the composites from various aspects, including mechanical properties, electrical and thermal conductivities, *etc.* Therefore, the preparation/combination processes play a crucial role in optimizing metal matrix composites. Taking copper-based materials as an example, the common preparation techniques include flake powder metallurgy [74], molecular blending method [75], spray pyrolysis (SP) [76] and thermal spraying method [77], as listed in Table 2.

### 2.2.1 Flake powder metallurgy method

Flake powder metallurgy process uses ball milling to suppress the agglomeration and promote uniform distribution of CQDs within metal matrix composites. By properly adjusting the rotation speed, milling time, and weight ratio of balls to composite precursors, grinding CQDs and metal-based powders with steel balls of different diameters can mechanically incorporate CQDs into the metal matrix, increasing the combination between metal and CQDs [78,79]. This process involves frequent cold welding, fracture and re-welding of powder particles [80]. During the preparation, the metallic particles are ground first into 2D slices, and their geometric shape is more in line with 1D CNTs [81]. This flake powder metallurgy technique can keep the intact structure and homogeneous distribution of carbon nanomaterials in the metal framework, and reduce the degree of work hardening of metal matrix composite powder, leading to the formation of metal matrix composites with high toughness. The flaky powder metallurgy method can also refine grains [82] and use the unique properties of carbon nanomaterials to produce ultrafine grained metal matrix composites. For example, Akbarpour et al. [83] successfully prepared ultrafine Al-CNT composite (2 and 4 vol.%) using sheet powder metallurgy method combined with hot pressing process. They conducted a comprehensive examination of the microstructural features and tribological behaviors of the resultant composite material (Figure 12). The results reveal undamaged structure and homogenous distribution of CNTs throughout the composite, alongside a reduction in both the friction coefficient and wear rate of aluminum, attributed to the reinforcement of the ultrafine grain matrix.

### 2.2.2 MLM

MLM was first used by Korean researcher Cha *et al.* for preparation of CNTs/copper matrix composites [84,85]. In that process, a mixture of sulfuric acid and nitric acid was

able 2: Example of recent metal matrix composites of CQDs and their preparation method

Туре	Fabrication method	Source	Strength enhancement	Performance enhancements	Ref.
Cu-CNT	Powder metallurgy method	Cu powder, multi- walled CNTs		Increase in wear resistance and microhardness	[46]
cQD/cu	Powder metallurgy method	СQD, Сu(СH₃COO) <sub>2</sub> ·H₂O	Tensile strength of the CQD/Cu composite materials Electrical conductivity of the composites remains and mechanical properties of the composite relatively high improved	Electrical conductivity of the composites remains relatively high	[72]
RGO/Cu	Molecular level mixing (MLM) and self-assembly	GO, Cu(СН <sub>3</sub> COO) <sub>2</sub> .H2O	Tensile strength is significantly higher than that of pure copper, toughness and strength improved compared to monolithic copper	Good electrical conductivity	[75]
CNTs/Cu-Ti	SP	CNTs, Cu (CH <sub>3</sub> COO) <sub>2</sub> ·H <sub>2</sub> O, Cu-Ti	Ultimate tensile strength(UTS) increase, yield strength (VS) increase, load transfer strengthening, and toughness improvement	Ductility improvement	[76]
CCTS: CQD ZVI@Fe₃O₄© CQDs	SP Electrodeposition and solvothermal	CQD, Cu₂CoSnS₄ FeSO₄, Fe₃O₄, CQD	More resistant to structural degradation under different reaction conditions	Good photo-response [86] Increasing the surface area, facilitating electron transfer [87] processes, promoting adsorption of reactant molecules, and extending the working pH range	[86]

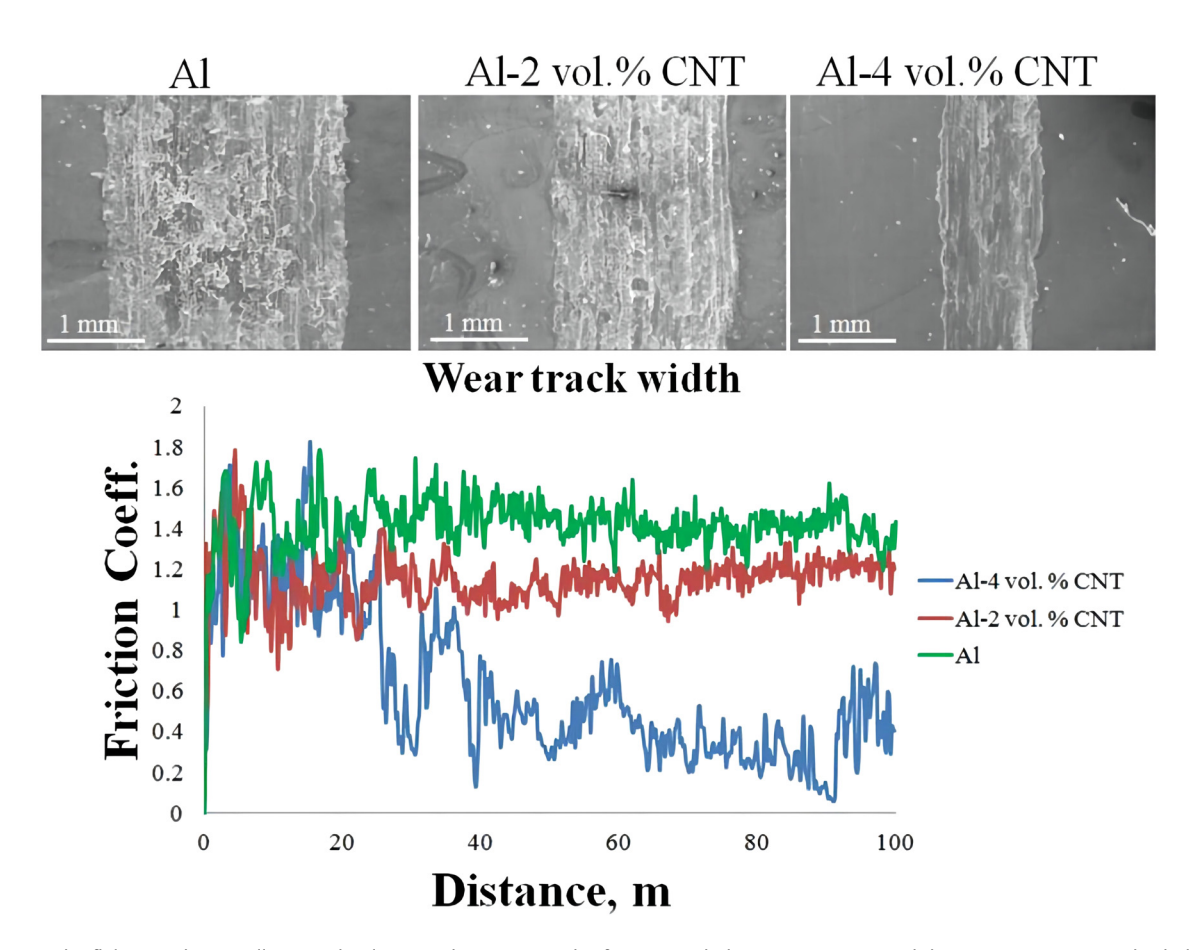


**Figure 12:** The flake powder metallurgy technology used to prepare ultrafine grained Al-CNT composites and their microstructure and tribological performance [83].

used to treat the carbon nanomaterial to generate surface defects and introduce oxygen-containing surface functional groups (e.g., hydroxyl, carboxyl, nitro, etc). Afterwards, the modified carbon material was added to a copper salt solution, where copper or cuprous oxide (Cu<sub>2</sub>O) particles were produced subsequently under certain conditions. After reduction of the system in hydrogen atmosphere, CNTs/copper matrix composite powder was finally obtained. The preparation of metal matrix composites by molecular blending method can greatly improve the dispersion degree of carbon nanomaterials in metal matrices. SEM measurements show that CNTs interpenetrate in the Cu<sub>2</sub>O structure and have strong interface bonding with the metal matrix. Hwang et al. [88] proposed a MLM process and a spark plasma sintering procedure for preparation of graphene-modified copper matrix nanocomposites. They studied the strengthening effect of graphene on the material. The preparation process is illustrated in Figure 13. The results demonstrate that using molecular level blending method can prevent the thermal damage of graphene sheets and improve their dispersion during the nanocomposite preparation process. Kim et al. [89] prepared CNTs-reinforced Cu

**DE GRUYTER** 

matrix nanocomposite with molecular blending method, and found that the thermal conductivity of the CNT/Cu composite decreased as the volume fraction of CNT increased from 5 to 10%, indicating that the CNT/metal interface formed by incorporation of CNTs can act as a thermal barrier to strengthen the metal matrix composite. Using MLM method to prepare CQDs/metal-based composites can reduce the heat loss of the materials and enhance their hardness. However, the drawbacks of MLM are low yield and cumbersome processes.

### 2.2.3 SP

SP refers to the process of spraying the solution of metal salt precursor into the SP furnace with low temperature heating in the atomizer to evaporate the precursor solution, and then decomposing the metal salt in the high temperature environment of the SP furnace to obtain the metal matrix composite powder precipitated from the precursor solution due to supersaturation [90]. Alternatively, the precursor solution is sprayed into a SP furnace for drying in a

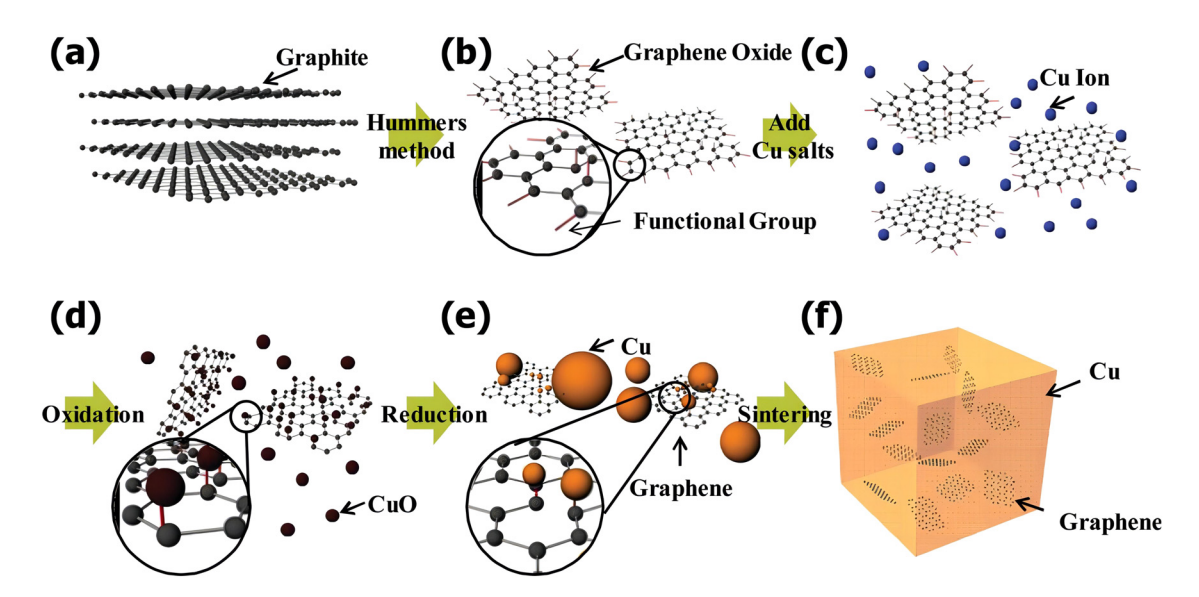


**Figure 13:** Schematic representation of the fabrication process for RGO/Cu nanocomposite. (a) Initial graphite material. (b) Graphene oxide synthesized using the Hummers method. (c) Homogeneous dispersion of Cu salt in graphene oxide solution. (d) Conversion of Cu ions to Cu-oxide on the surface of graphene oxide. (e) Reduction process involving both Cu-oxide and graphene oxide. (f) Formation of sintered powders comprising RGO/Cu nanocomposite materials [88].

high-temperature atmosphere, and then heat treated to form the powder product. In this synthesis, composite powder samples with different particle sizes and uniform dispersion can be easily obtained by adjusting the process parameters. Yang et al. [91] synthesized CoTe2-C composite microspheres by SP (Figure 14). Because of the convenient direct incorporation of Te into the composite microstructure, only a simple one-step post-treatment process was required to produce the CoTe<sub>2</sub>-C microspheres with pure phase and uniform composition. CQDs-reinforced Co matrix composites were also prepared by SP, which improved the cycle stability and magnification properties of the composites. Zhang et al. [92] synthesized CNT-tungsten (W) composite powder with an interconnected structure by SP, and further prepared CNT-W/Cu composites. Characterization results show a uniform dispersion of the W-containing CNTs in Cu matrix. Besides, it was found that the W particles are used to "pin" the CNTs. Based on the analyses of the CNT-W/Cu composite materials with respect to their interface

microstructure, mechanical properties, and conductivity, enhanced UTS and conductivity were observed for CNT-strengthened Cu-based materials. Therefore, the main advantages of the SP method in preparation of CQDs strengthened metal matrix composite are simple processes from precursor solution preparation to powder generation, and high synthesis capacity, which can meet the needs of large-scale production.

### 2.2.4 Thermal spraying method

Thermal spraying is a technique to protect and strengthen the surface of metal matrix composites [93]. In a typical process, the coating material is heated to a (semi-) molten state by a heating source (*e.g.*, combustion flame, plasma arc, *etc.*), and then sprayed onto the pretreated metal matrix surface with the help of the power of flame flow or the impact of high-speed inert gas flow. By this means, a

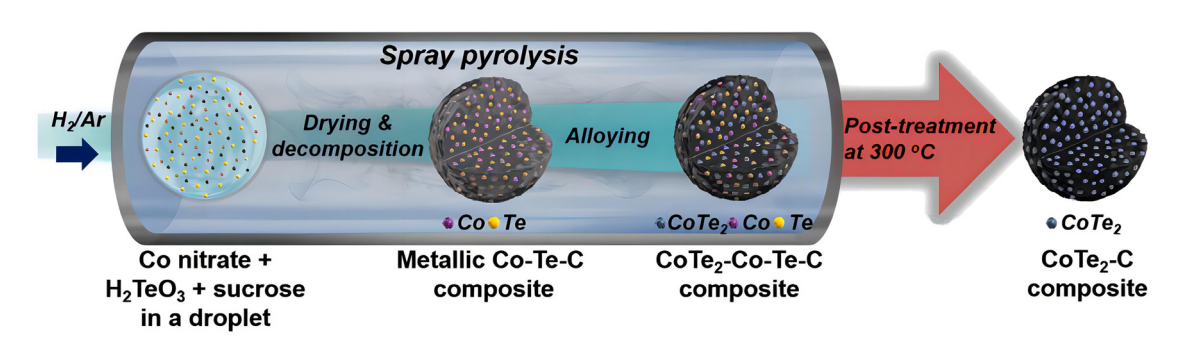


Figure 14: The synthesis process of CoTe<sub>2</sub>-C composite [91].

solid covering layer of the coating material on the metal substrate is formed, and special functions of the composite material could be expected [94]. The advantages of the thermal spraying process are its simplicity, flexibility, and high efficiency. Besides, it was reported that the wear resistance of the metal matrix composites prepared by this method was improved by 200–400% [95]. However, this process is limited to small quantity sample preparation, and not capable for large-scale production of the composite materials.

#### 2.2.5 Other methods

In addition, some researchers mixed CQDs and metal oxides under sonication to prepare CQDs-reinforced metal matrix composites. As shown in Figure 15, Elugoke *et al.* [96] prepared CuO NPs by chemical precipitation method and combined them with CQDs, which were synthesized *via* pencil graphite carbonization in accordance with the Hummer approach used by Algarra *et al.* [97]. In the synthesis process of CQDs/CuO nanocomposites, CuO NPs and CQDs (each of 4 mg) were added into a glass container with 0.2 mL of dimethylformamide. Then, perform ultrasonic treatment on the mixing system in a water bath at 25°C. The resulting paste was used to modify GCE by dropping. The sensitivity of CQD modified GCE is ten-fold higher than the corresponding value of the bare GCE. Huang *et al.* [98] synthesized composite materials of CQDs and chitosan

(CS) under intense sonication and found that CQDs and CS were uniformly mixed in the composite materials. The composite modified GCE (CDs CS/GCE) exhibits good response to DA with a detection limit of 11.2 nM.

In summary, there are many preparation methods for CQDs and their reinforced metal matrix composites, and each has its advantages and disadvantages. Therefore, when preparing the abovementioned materials, the appropriate methods should be selected according to their characteristics and the product requirements. The commonly used organic precursors for preparing CODs are citric acid and sugar. The commonly adopted preparation methods include hydrothermal method, microwave assisted synthesis, and thermal cracking method, while the arc discharge method is rarely used because its products have complex composition and they are difficult for separation and purification, resulting in low yield of this method. Due to the cumbersome process, the laser ablation method also has very limited application. Both the precursor material and the preparation method have significant influences on the structural characteristics and practical performances of the as-obtained CQDs. There is very limited research on the correlation between the structures and properties of CQDs. Future research work should focus on design of novel preparation routes using organic precursors and advanced technologies, as well as investigation of the correlation between preparation conditions, structural characteristics, and practical performances of CQDs (Figure 16).

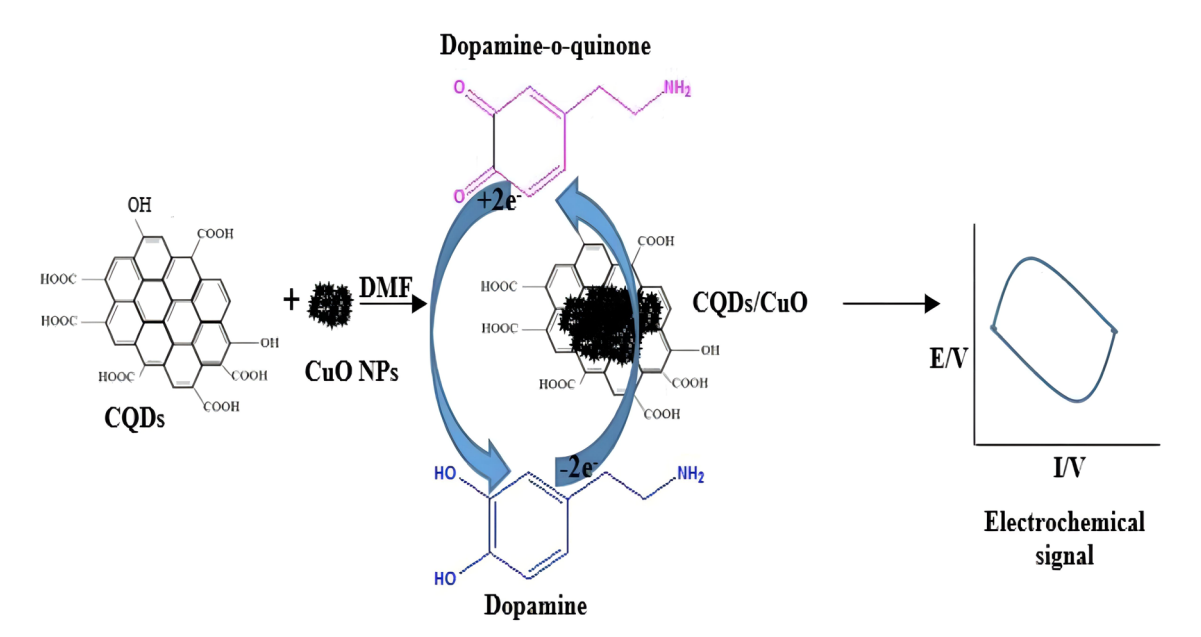


Figure 15: Preparation of CQDs/CuO nanocomposites from pencil graphite precursor [96].

### 2.3 Dispersion of CQDs in metal matrix composites

Metal matrix composites-reinforced with CQDs are garnering significant interest due to their superior comprehensive performances. The degree of dispersion of CQDs in the metal matrices is a critical determinant of the extent to which the properties of the composites are improved [99,100]. Especially, it strongly influences the mechanical properties of metal matrix composites. Well-dispersed CQDs are more likely to exert a reinforcement effect on the composite material.

The methods for dispersion of CQDs into metal matrix composite materials can be divided into physical dispersion methods, chemical dispersion methods, and so on. The effect of different dispersion methods on the structural characteristics of CQDs varies, and the method selection should be based on the requirements of actual applications.

### 2.3.1 Physical dispersion methods

The physical dispersion methods mainly apply mechanical equipment to disperse agglomerated CQDs through physical interactions. They have the advantages of simple process, convenient operation, and the avoidance of impurity introduction. The relevant techniques include ultrasonic dispersion, high-energy ball milling, and post-treatment technology. The ultrasonic method is often used for predispersion of CQDs. In a typical process, CQDs are mixed with organic solvents and treated under ultrasonication to break the CQD agglomerates before processing in the next step of treatment or application. Wang *et al.* [101] used the ultrasonic dispersion method to prepare a suspension of CQDs by mixing CQDs, anhydrous ethanol, and wetting

dispersant under ultrasonication. Afterwards, aluminum sheets were immersed in the suspension and subjected to both ultrasonication and heat treatments until anhydrous ethanol completely evaporated, resulting in a uniformly dispersed CNTs on the aluminum substrate. Besides, highstrength carbon nanomaterial-reinforced metal matrix composites have also been prepared by cumulative rolling welding. The high-energy ball milling method is widely used for dispersion of CQDs. Through the collisions between powders, grinding balls, and milling tanks, the CQD agglomerates can be crushed into fine powders and dispersed into other media. Chen et al. [102] used high-energy ball milling to mix carbon nanomaterials and aluminum powder, and successfully achieved uniform dispersion of the carbon nanomaterials on the surface of aluminum powder. After high-energy ball milling for 48 h, the tensile strength of the resulting Al-1% composite-reinforced by carbon nanomaterials reached 368 MPa.

In addition to the above dispersion methods of CQDs in mixed powder, appropriate post-treatment techniques can also effectively improve the dispersion of carbon nanomaterials. For example, post-processing technologies such as high-pressure torsion, hot extrusion, and equal diameter angular extrusion can refine and homogenize the microstructure of composite materials under strong external forces, and use shear force to break the CQD aggregates, fully leveraging the strengthening effect of carbon nanomaterials. Tan et al. [103] synthesized N-doped CQDs using isophorone diisocyanate as a single carbon source under microwave radiation. In addition, the obtained N-doped CQDs can be uniformly dispersed in various organic monomers in the absence of organic dispersants, resulting in a polyurethane composite material loaded with well-dispersed CQDs.

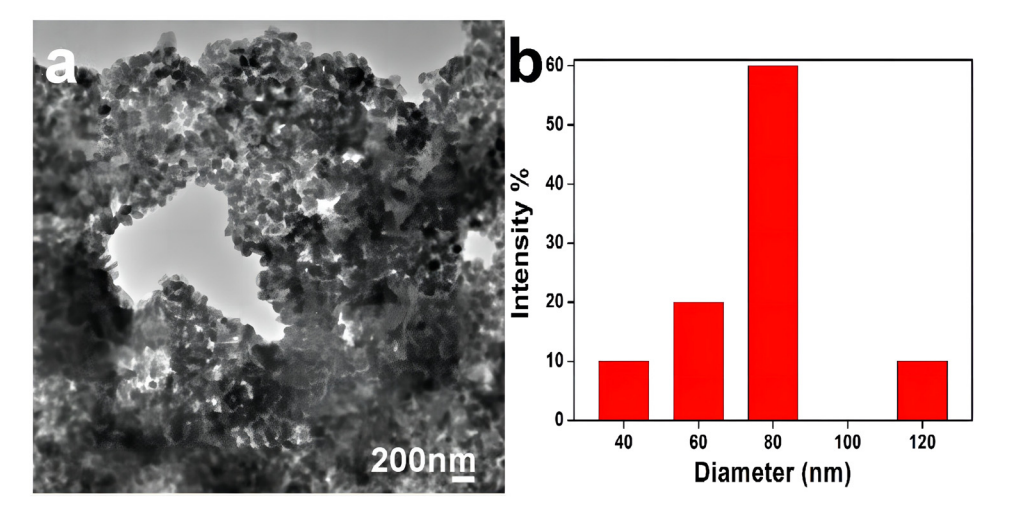


**Figure 16:**  $CuS_x$  NPs: (a) TEM image and (b) size distribution diagram. [104].

### 2.3.2 Chemical dispersion methods

The chemical dispersion methods mainly break down the CQD agglomerates through chemical reactions, which can ensure the structural integrity of CQDs. They mainly include the *in situ* synthesis methods, PVP pyrolysis methods, surface modification methods, *etc*. The *in situ* synthesis method is the direct formation of CQDs on the surface of metal powder or metal matrix through chemical reactions. The *in situ* synthesized CQDs usually show good adhesion with the metal matrices and uniform dispersion in the composites. As the most mature method of *in situ* synthesis, chemical vapor deposition is widely used in the preparation of well-dispersed CQD systems.

The polymer pyrolysis method is the decomposition of a polymer mixed with CQDs and metal powder under heat treatment to prepare CQDs/metal composite powder. The commonly used polymers are poly butyl acetate (PBA), polyvinyl alcohol (PVA), and PEG. Huang *et al.* [104] prepared CQDs/CuS $_X$  NPs using thermal dodecyl mercaptan pyrolysis method and investigated the role of CQDs in the preparation process. The results indicate that CQDs can effectively improve the dispersion of CuS $_X$  particles and reduce the size of CQDs/CuS $_X$  composites. This may be due to the structural characteristics of the small size and good dispersion of CQDs, leading to the formation of many crystal

nucleuses in the initial reaction stage. On the one hand, the small size of CQDs means a high specific surface area, making them extremely reactive in chemical reactions, thus promoting the formation of crystal nucleuses. On the other hand, the good dispersion makes the CQDs show a non-uniform distribution in space, forming many small local regions, which is easier to promote the formation of crystal nucleuses during the reaction process, and further increases the number of crystal nucleuses. The formation and evolution of these crystal nucleuses are of great significance for the preparation of CQDs materials with excellent properties.

The inherent poor wettability of CQDs with metal substrates presents challenges in achieving strong CQD—metal bonding and high CQDs dispersion within the metal matrix using conventional methods. Surface coating and modification of CQDs can significantly improve their wettability with the metal matrix, thereby enhancing CQD dispersion. Li *et al.* [105] prepared ruthenium-based composite materials reinforced with CQDs by loading ruthenium NPs onto CQDs (Ru@CQDs). Characterization results show that the strong coordination interaction between the d-orbitals of Ru and the functional groups on the surface of CQDs successfully anchored Ru NPs on the surface of CQDs, which prevents CQDs from aggregation, resulting in highly dispersed Ru@CQDs composite NPs (Figure 17).

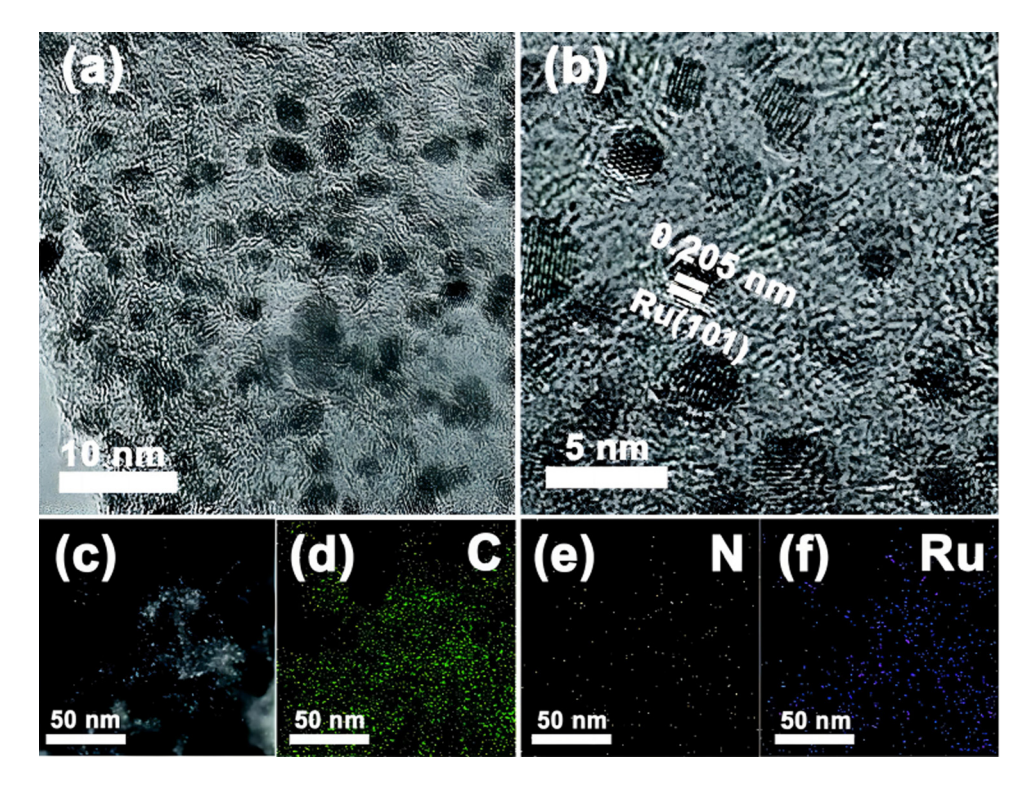


Figure 17: (a) TEM, (b) HRTEM, and (c) HAADF-STEM images of Ru@CQDs with corresponding EDX elemental mapping of (d) C, (e) N, and (f) Ru [105].

## 3 Effect of CQDs as reinforcement phase on the interface of metal matrix composites

### 3.1 Wettability of CQDs/metal interface

The interface is an important microstructure of composite materials, and the improvement in the composite material performances can only be achieved by enhancing the interface bonding states between reinforcement agents and matrices. The strength of this interfacial bond is crucial in determining the ultimate performance of CQDs-reinforced metal matrix composites. Furthermore, the wettability between CODs and metal is a fundamental factor influencing the interfacial bonding strength within these composites. Therefore, by regulating the wettability of the reinforcement agent and matrix, the comprehensive performance of the composite material can be improved. At present, the main problem lowering the performance of CQDs-reinforced metal matrix composites is the poor wettability of the CQDs/metal interface, resulting in weak interfacial bonding strength.

Wettability refers to the ability of a liquid to automatically spread on the surface of a solid due to surface tension difference. For example, if droplets aggregate into spherical shapes on a solid surface without spreading, this phenomenon is called poor wettability or non-wetting. On the contrary, the phenomenon that droplets spread on a solid surface without maintaining spherical shrinkage is called wetting [106,107]. Wettability corresponds to a capillary system, where the wetting of the inner wall of the solid phase by liquid is the contact angle between the capillary rising and the solid-liquid interface. A contact angle below 90° indicates that the solid-liquid phases are wet, and the liquid can spontaneously penetrate into the pores under the driving force of capillary action. Generally speaking, smaller contact angle suggests better wettability, and better interfacial bonding between the two phases [108].

For metal matrix composite reinforced by CQDs, the interfacial wettability between CQDs and metals is the core factor in improving their performance. Based on whether the metal melt reacts with the CQDs matrix, reactive and non-reactive wettings could be determined. Non-reactive wetting is mainly caused by Van der Waals force between metal melt and CQDs matrix, which belongs to physical combination, so the binding force is very weak. In the reactive wetting system, the metal melt undergoes dissolution, diffusion, and chemical reactions with the CQDs matrix, leading to complex spreading kinetics. The generation of new compounds at the metal/

CQDs interface results in complex structures and compositions of the composite material. The chemical reactions at the interface could improve the wettability of the system, which is because the generated interface reaction layer is usually more metallic and has better compatibility with metals. Moreover, the chemical reaction process can also reduce surface energy at interface and promote the system wettability [109].

Therefore, improvement in the wettability between reinforcement agent and metal matrix is an efficient route to prepare CQDs-reinforced metal matrix composite with excellent performances. Currently, there are two effective ways to improve the wettability between CQDs and metal matrix.

1) Active metal alloying method. By introducing elements that can be alloyed with the matrix and simultaneously have good wettability with the reinforcement agent, the compatibility between the different components can be significantly improved. Mao et al. [110] studied the wettability of copper and titanium at different positions with C at 1.373 K, and found that the system Cu/Ti/C has best wettability than Ti/Cu/C, and Cu-Ti/C shows the lowest wetting ability. This is due to the different contact areas between liquid phase Cu-Ti and C matrix in the heating process. Figure 18 shows the microstructure of the interface layers at three different placement positions. For all three systems, continuous reaction layers are formed at the metal/carbon matrix interface, and their thickness varies at different placement states. The thickness at placement positions b and c is larger than that at placement position a. The difference in thickness indicates that the larger the contact area between Ti and the carbon matrix, the more intense the interface reaction. Mortimer and Nicholas [111] investigated the wettability of Cu alloys on amorphous carbon surfaces with relatively low Cr content. The results showed that at Cr content of 0.1 mol%, the equilibrium contact angle was 128°, which decreased to 45° with the increase in the Cr content, indicating that the wettability of carbon/ copper system could be effectively improved by increasing the Cr content.

Wan *et al.* [112] studied the alloying effect on the interface state between carbon and copper, and also found that higher Fe/Ni content in Cu alloys results in larger contact area between them and carbon materials, *i.e.*, smaller contact angle. Kishkoparov *et al.* [113] found that after thermal treatment of the system at 1,523–1,823 K, a large amount of CoC formed at the interface of Cu–Co/C systems. The results indicate that the carbide interface promotes the wetting. The same finding was also reported by Naidich and Kolesnichenko in 1968 [114]. Yang *et al.* [115] found that increasing the Cr content in the alloy could improve

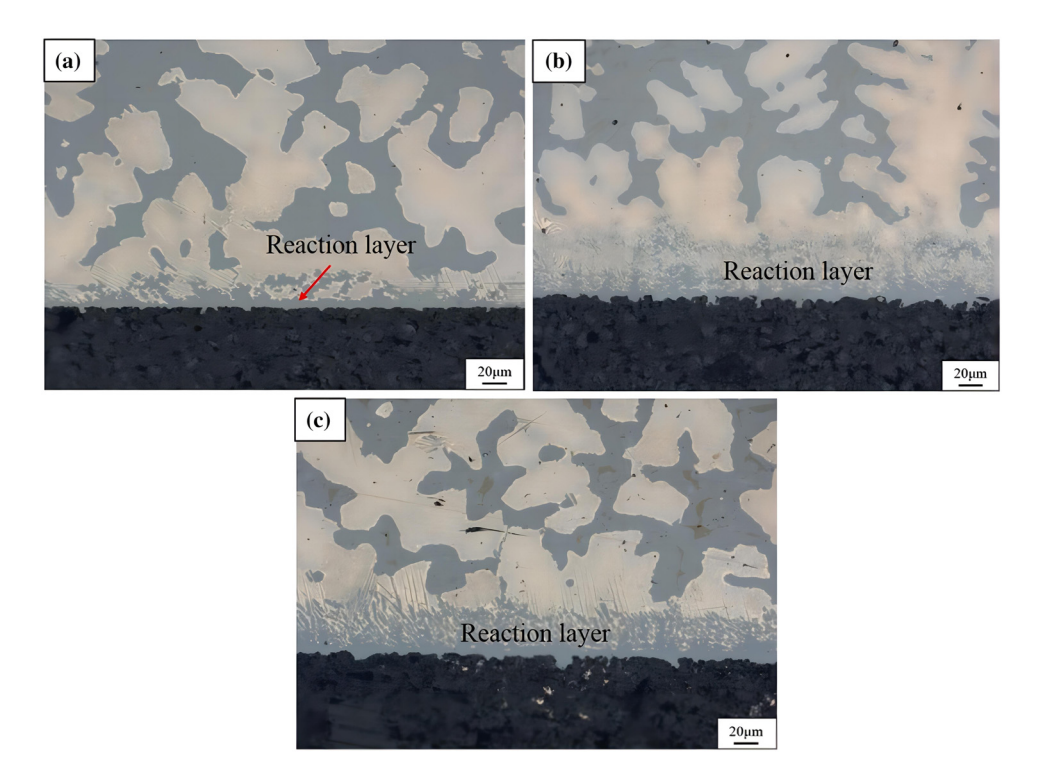


**Figure 18:** Cross-section micrographs of Cu-10 mass percent Ti alloy/graphite in three kinds of placement states after 1 h at 1,373 K (1,100°C) (the Cu–Ti alloy is above, and the graphite substrate is below): (a) placement state A; (b) placement state B; and (c) placement state C [110].

the wettability, which can be attributed to the transformation of  $Cr_3C_2$  at the interface to a more wettable metalloid  $Cr_7C_3$  (Figure 19).

2) Reinforcement surface modification method. It is a widely used technique based on the principle of changing the interface energy of the solid phase. Metals have good compatibility between each other, and if liquid metals have a certain solubility with active metals or form intermetallic compounds, their wettability can be effectively improved. Therefore, synthesis of a metallic coating layer at the surface of solid reinforcement agent can promote the liquid to penetrate into the reinforcement agent. Zhang et al. [116] carried out the chemical synthesis of carbides

of Co and W with different Ru additions on the carbon phase surface to enhance the interface connection of Co/C, and found that Ru could inhibit the abnormal growth of WC grains and the mean grain size of WC grains decreases, improving mechanical properties and cutting performance of WC-8Co.

Yang *et al.* [117] used W as a coating material and produced a thin WC intermediate layer on the C surface (Figure 20). The unmodified C showed poor wettability with copper particles, and the copper particles contracted into spherical bodies, which could not be spread on the C surface. After modifying C with W element, copper particles achieved good spreading on the C, indicating that the

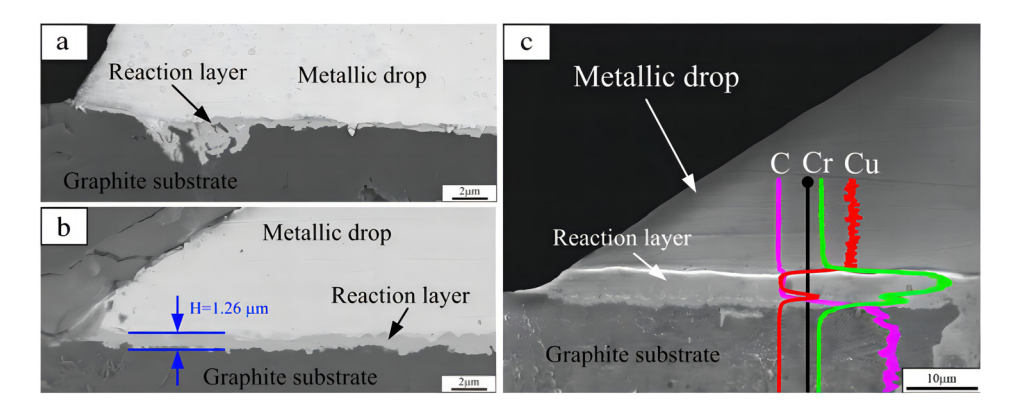


Figure 19: Back-scattered electron images of the microstructures at the triple junctions of the wetted Cu–Cr/C samples at 1,373 K: (a) 0.5 at.% Cr for ~40 min; (b) 1.0 at.% Cr for ~30 min, and (c) 2.0 at.% Cr for ~40 min [115].

introduction of WC intermediate layer can indeed change the wettability of carbon/copper and increase the interfacial adhesion between carbon and copper.

CQDs are a type of zero-dimensional carbon nanomaterials with ultrafine quasi-spherical particles below 10 nm. They are usually composed of amorphous and crystalline carbon with different oxygen-containing functional groups on the surface, such as hydroxyl and carboxyl groups. Many researchers claim that CQDs contain sp<sup>2</sup> crystalline carbon, but the crystallinity is poor. There are many defects at the edges of CQDs, while the core has a crystalline structure similar to graphene. Previous studies have shown different core structure models of CQDs, such as diamond-like structure, graphite oxide like material, and amorphous carbon [118,119]. In addition, CQDs frequently undergo  $n \to \pi^*$  and  $\pi \to \pi^*$  electronic transitions. The  $\pi$  state of CQDs is generated by sp<sup>2</sup> hybridized carbon atoms in the carbon nucleus. In the  $\pi$  state, the band gap gradually decreases with the increase in aromatic rings, which only occurs in  $\pi$  conjugated organic molecules. The nstate of CQDs is generated by lone pair electrons in oxygencontaining functional groups. If lone pair electrons exist in oxygen-containing functional groups, their orbitals will conjugate with sp<sup>2</sup> hybridized carbon atoms, and electrons will transfer from the n-state in oxygen-containing functional groups to the  $\pi^*$  state in aromatic rings [120]. Due to the above structural characteristics of CQDs, CQDs-reinforced metal matrix composites usually show higher wettability and better alloying process compared to metal matrices reinforced by other carbon nanomaterials.

### 3.2 Interface bonding strength

The performance breakthrough of CQDs-reinforced metal matrix composite mainly faces three challenges: (1) Achieving uniform dispersion of CQDs; (2) improving the interface effect between CQDs and metal substrates; and (3) ensuring the structural stability of CQDs. The bonding interface between CQDs and metal matrix plays a crucial role in the performances of the composite materials. Aiming at improving the interface effect between CQDs and the metal substrate, surface modification, surface coating treatment, alloy element catalysis, and preparation process optimization can be conducted.

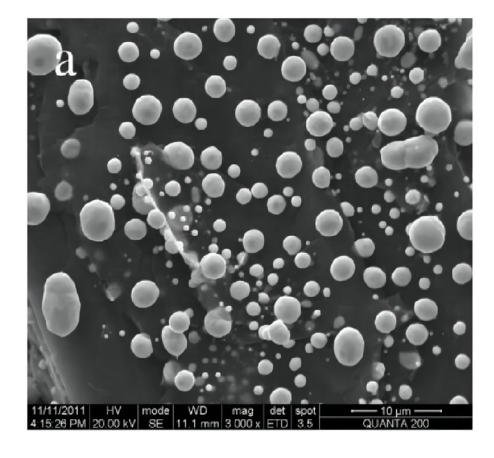
To achieve the above target, the interface bonding strength needs to be determined. Chu *et al.* [13] introduced a method to calculate the interface bonding strength through the interfacial shear mechanism. The formula is shown below.

$$\sigma_{\rm c} = \frac{1}{2} \tau_{\rm ISS} p f_{\rm g} + \sigma_{\rm m} (1 - f_{\rm g}), \quad p < p_{\rm c},$$
 (1)

where  $\sigma_{\rm c}$  and  $\sigma_{\rm m}$  represent the tensile strength,  $\tau_{\rm ISS}$  represents the interfacial shear strength, which can be considered as the interface bonding strength in this condition.  $f_{\rm g}$  represents the volume percentage of CQDs, p represents the aspect ratio of CQDs, and  $p_{\rm c}$  represents the critical aspect ratio of CQDs. This formula can be converted into the following form for calculation of the interface bonding strength:

$$\tau_{\rm ISS} = 2 \frac{(\sigma_{\rm C} - \sigma_{\rm m})/f_{\rm g} + \sigma_{\rm m}}{p}.$$
 (2)

Hwang *et al.* [88] proposed a MLM method to prepare copper/graphene composites, conducting tensile tests with an Instron Model 8848 microforce testing system. By adding functional groups onto the graphene surface, they successfully solved the dispersion issue of graphene within the Cu matrix, bolstering the interfacial bonding strength between graphene and Cu. Sayyad *et al.* [121] first modified the reduced graphite oxide (rGO) using Ag NPs by *in situ* chemical reduction. Ag NPs were uniformly spread over rGO



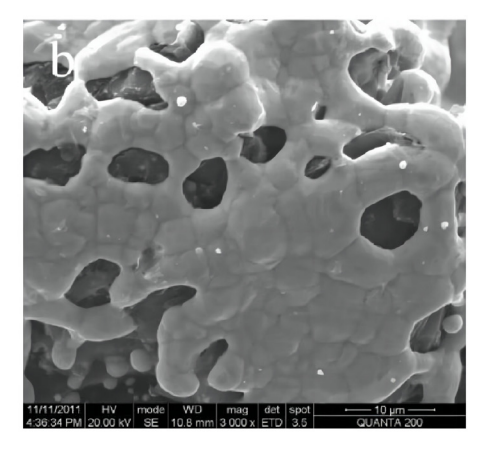


Figure 20: Cu coating dehumidification or spheroidization: (a) raw graphite and (b) W pre-coating [117].

surface acting as a spacer, which induced a transition of the graphene from a stacked state to a stripped state, effectively preventing the graphene nanosheets from agglomeration. The Ag NPs in the Ag/rGO reinforcement phase enhance the interfacial adhesion and react with the Cu matrix to form Cu–Ag bonds, thereby strengthening the composite material.

Furthermore, Ye et al. [122] prepared CQDs with diphenylamine structure attached to the surface by one-step pyrolysis method, and used them for strengthening steel to form metal matrix composite. Polar CQDs can be deposits on the interface as bearing balls to form an uneven protective film. CQDs have a good bonding interface with the metal matrix, demonstrating their excellent performance for friction reduction. Kong et al. [123] explored how carbon-based nanomaterials impact the thermal conductivity of Cu/Cr alloys. The results from microstructure and thermal conductivity characterizations showed that Cr<sub>2</sub>C<sub>3</sub> was generated at the interface between carbon and the metal matrix, which improved the C/metal-matrix interface bonding, leading to an enhanced thermal conductivity of this composite material. Cho et al. [124] introduced carbon nanomaterials into copper matrix as reinforcement components through powder metallurgy to prepare CNT-Cu composites with good thermal conductivity. The thermal conductivity test and microstructure characterization of the composite material indicated that the homogeneous dispersion and strong interfacial bonding of carbon nanomaterials within the copper matrix play crucial roles in improving its thermal conductivity.

### 3.3 Functionalization of the reinforcement

CQDs are usually 2-10 nm sized carbon nanomaterials composed of sp<sup>2</sup> hybrid graphite cores with polar oxygen groups. Because the carbon point surface contains a huge quantity of the oxygen-containing functional groups (such as amino, carboxyl, hydroxyl, etc.), it shows excellent water solubility and, in most cases, it is in a uniformly dispersed status, which also provides the possibility for different types of surface functionalization. Because carbon atoms are in a disordered state, they often show amorphous structure [125]. Generally, the carbon point contains chemical bonds including C-H, C=O, C=C, -OH, and may also have C-N, N-H, and C-S bonds. The Raman spectrum of CQDs shows three main peaks (Figure 21), in which the D and G peaks are mainly correlated with the strength and defect degree of the prepared carbon point. They are centered at 1,350 and 1,580 cm<sup>-1</sup>, respectively, while the 2D peak is around 2,700 cm<sup>-1</sup>. The intensity ratio of the D

and G peaks is ca. 0.32. The X-ray Photoelectron Spectroscopy (XPS) spectrum in Figure 22a presents three distinct peaks at 285, 400, and 530 eV, corresponding to C1s, N1s, and O1s, respectively. The four peaks on high-resolution C1s spectrum (Figure 22b) indicate the presence of C-C, C-N, C-O, and C=O bonds. The two peaks on N1s spectrum (Figure 22c) demonstrate the existence of C-N-C and N-H bonds. The FTIR spectrum in Figure 22d showcases characteristic bands for -O-H and -N-H stretching vibrations in the region of 3,200–3,400 cm<sup>-1</sup>. The 1,656 cm<sup>-1</sup> peak is tied to carbonyl stretching, and the one around 1,340 cm<sup>-1</sup> is linked to C-N stretching vibration. Peaks at 1.618 and 1.533 cm<sup>-1</sup> are associated with C=C stretching in polycyclic aromatic hydrocarbons, indicating the presence of sp<sup>2</sup> hybridization. Additionally, peaks at 1,124 and 1,050 cm<sup>-1</sup> are derived from C-O bonds vibration in the carboxyl group. These findings indicate that the CQDs contain various functional groups including -OH, -COOH and -NH, which significantly enhance their water solubility. The effects of CQDs on the interface of the metal matrix composites are mainly reflected in the interface morphology, functional groups, phase structure, potential, and so on.

He *et al.* [126] successfully constructed a novel ternary nanocomposite material MIL-53 (Fe)/CQDs/metal nanoparticles (MNPs) (MNPs = Ag, Pd, Au) through a simple two-step procedure containing the self-assembly and the *in situ* photoreduction. It was observed that the composite material has excellent photocatalytic activity, possibly because of the improved light absorption intensity and excellent conductivity of CQD, as well as surface plasmon resonance effects of Au. The results from XRD, FT-IR, UV-vis, and

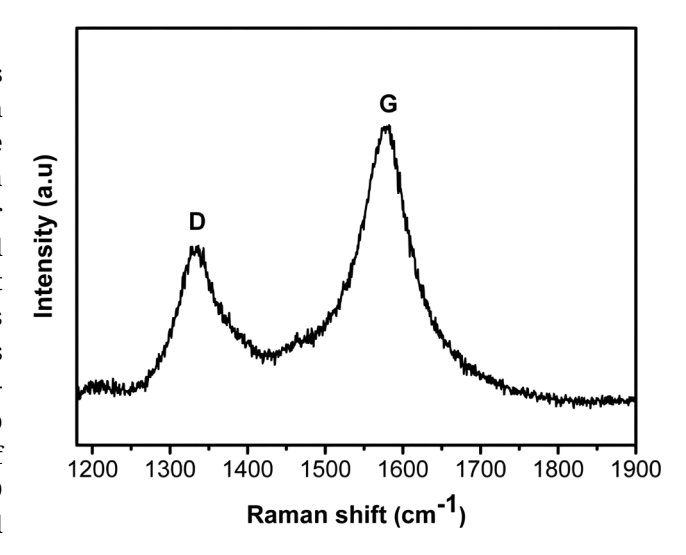


**Figure 21:** Raman spectrum of CQDs. The D bands are involved with the defected carbons, and the G bands come from the graphitic in-plane vibrations of ideal sp<sup>2</sup> carbons [125].

22 — Yuting Xie et al. DE GRUYTER

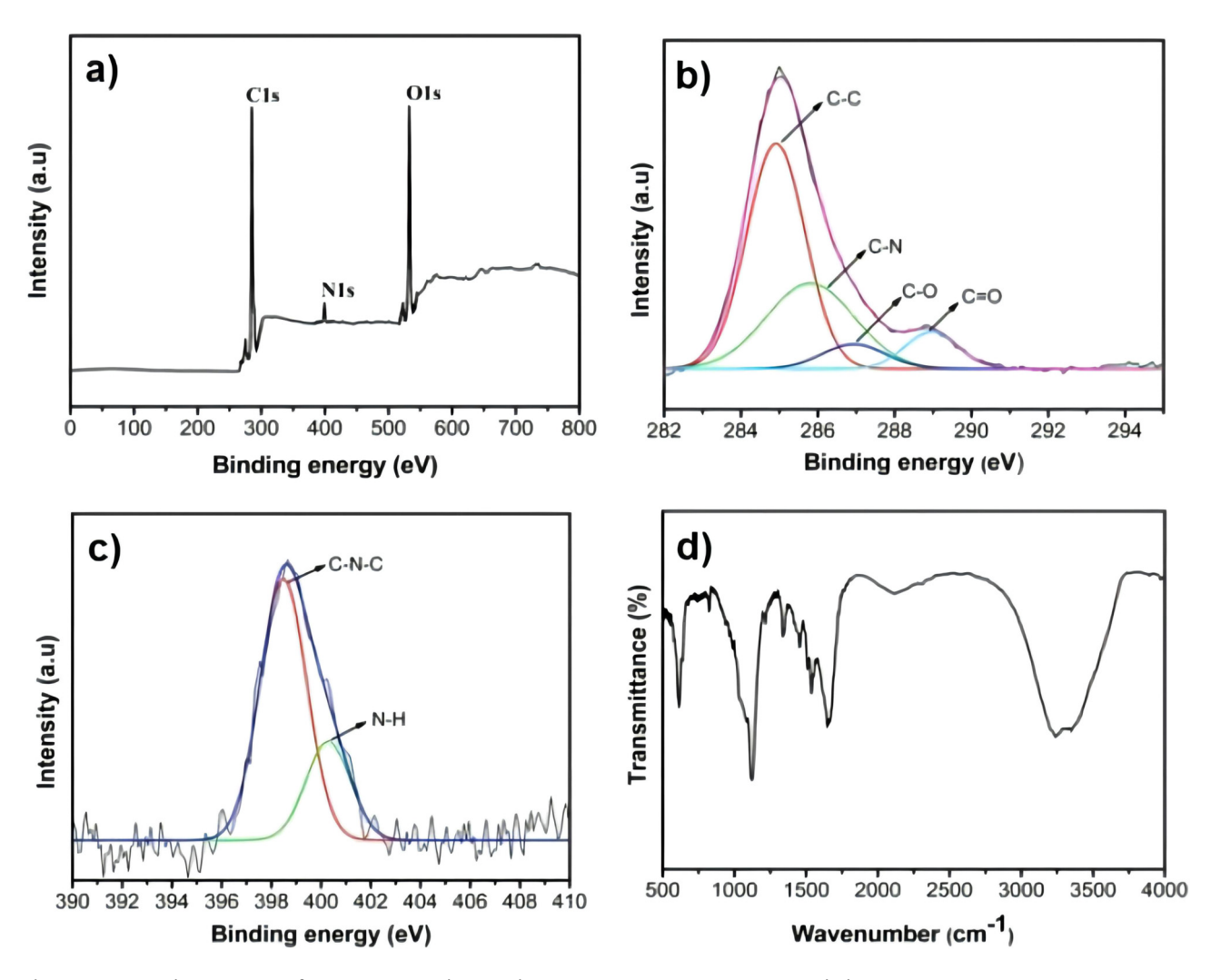


Figure 22: XPS and FTIR spectra of CQDs. (a) XPS wide scan; (b) C1s spectrum; (c) N1s spectrum; and (d) FTIR spectrum [125].

potential analyses show that after the reinforcement of metal matrix materials with CODs, MIL-53 (Fe) still maintain good integrity with undamaged structure (Figure 23). However, the reinforcement phase of CQDs affects the interfacial bonding of metal matrix composites, and the functional groups (such as OH, COOH, etc.) on the CQDs surface contribute to the better electrical and mechanical properties of the composites. Fan et al. [127] used CQDs to activate MOFs and applied them for detection of Fe<sup>3+</sup> and Cu<sup>2+</sup> (Figure 24). Analysis results reveal a hydrogen bond interaction between CQDs and MOFs in the composite, suggesting that CQDs/MOFs composites are not a simple physical mixture of CQDs and MOFs. Due to the abundant functional groups on the CQDs surface, the mechanical, thermal, and electrical characteristics of the composite interface have been affected.

The organic functional groups (*e.g.*, –OH, –COOH, –NH<sub>2</sub>, *etc.*) on the CQDs surface can provide more active sites and

binding sites for preparation of multicomponent and highperformance metal matrix composites [64,128,129]. More importantly, heteroatoms doped with multicomponent CQDs (N, S, P, B, etc.) can also promote electron transfer through internal interactions, thereby improving the electrical properties of composite materials [130]. In addition, strong interfacial interactions within multicomponent nanocomposites can further promote intermolecular electron transfer, which is highly important for optimizing the electrical properties of metal matrix composites [131]. Most of the previous studies on CODs-modified composite materials aimed at improving their photocatalytic and biosensory properties, while the research work focusing on the electrical, mechanical, and thermal performances of the composite materials was very limited. Recently, CQDs have begun to be widely used for enhancing electrical performance in the fields such as metal air batteries, fuel cells, and water cracking [132-134].

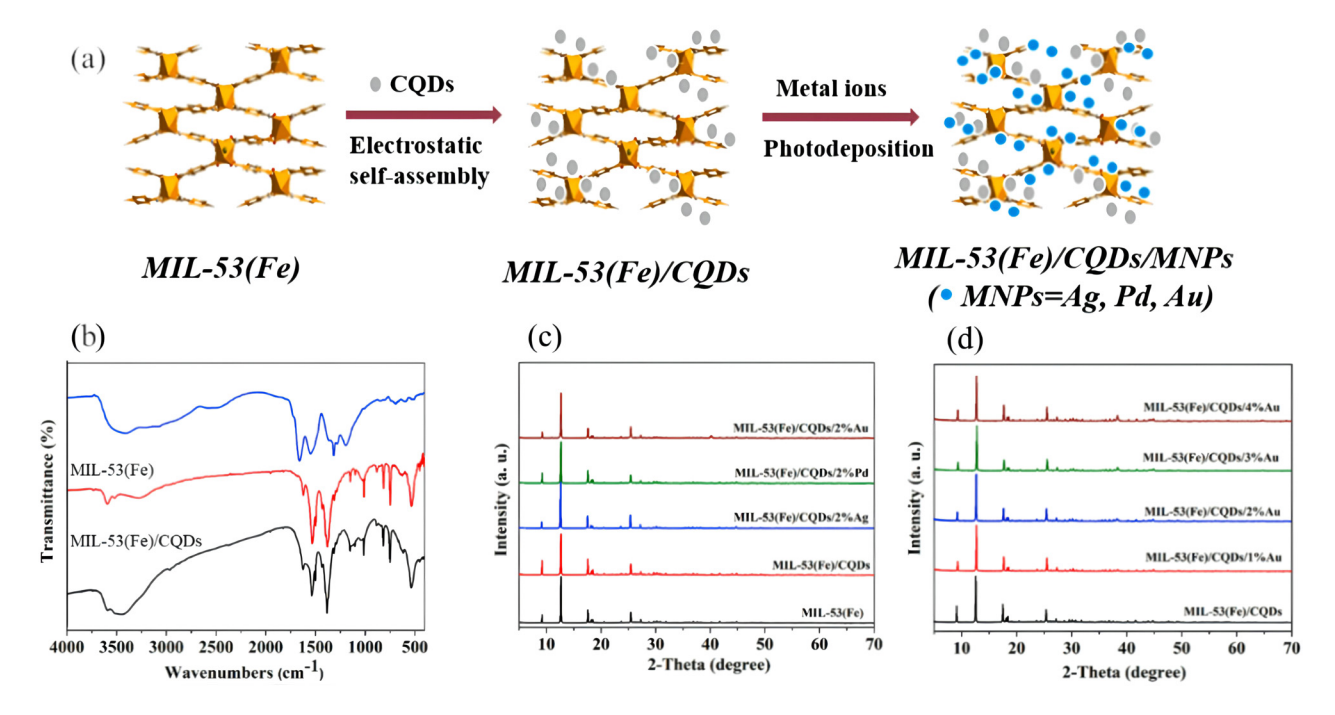


Figure 23: (a) The flow fabrication diagram of MIL-53(Fe)/CQDs/MNPs (MNPs = Ag, Pd, Au) samples, (b) FTIR spectra, (c) XRD patterns of MIL-53(Fe), MIL-53(Fe)/CQDs, MIL-53(Fe)/CQDs/MNPs, and (d) XRD patterns of MIL-53(Fe)/CQDs/Au with different contents of Au [126].

Except for high electron transfer capability and superior conductivity, CODs are also broadly used for fabricating multicomponent materials because their abundant functional groups (e.g., -OH, -NH2, -COOH, etc.) provide a wealth of advantageous sites [135]. Usually, these functional groups on the CQDs surface could efficiently coordinate with the metal ions containing vacant d orbitals to form stable CQD/metal coordination complexes [105]. More importantly, CQDs in metal matrix composites can limit metal NPs to form stable nanocrystals, preventing their aggregation and further growths [136]. Therefore, combination of metal NPs and CQDs is a promising way to design and develop stable metal matrix nanocomposites. Based on this strategy, a microwave assisted synthesis method with simple process was developed for the first time by our group and used to prepare flower-shaped MnO2 nanoscale catalysts supported on N-CQDs [20]. The addition of N-CQDs improves the catalyst conductivity, and also efficiently enhances the MnO<sub>2</sub> specific surface area (SSA) by splitting the MnO<sub>2</sub> nanoflowers into smaller ones with increased surface roughness. In addition, the influence of CQDs on the interface of metal matrix composites is also reflected in the PL intensity increase and the surface morphology change. Raikwar [137] synthesized CQDs using aloe biomass through a simple carbonization process, and found that the as-prepared CQDs can be applied in biological imaging of the plant cells and in safe printing with the CQDs ink. In addition, they also prepared

CQDs@LaPO<sub>4</sub> Eu<sup>3+</sup> nanocomposites. The strengthening effect of CQDs enhanced the PL intensity of the metal matrix composite interface, which could be explained by the Förster resonance energy transfer from the CQDs to Eu<sup>3+</sup>. Jing *et al.* [138] prepared Mn<sub>3</sub>O<sub>4</sub> composite materials (Mn<sub>3</sub>O<sub>4</sub>/C<sub>dots</sub>) coated with CQDs through green AC voltage electrochemical methods for the first time (Figure 25). Interestingly, the Mn<sub>3</sub>O<sub>4</sub> particles within the composite material show an octahedral morphology (Figure 25b and c). In the aspect of performance, the Mn<sub>3</sub>O<sub>4</sub>/C<sub>dots</sub> composites exhibit excellent electrochemical properties (Figure 25e).

### 4 Properties of CQDs-reinforced metal matrix composites

### 4.1 Mechanical properties and its reinforcement mechanisms

Some drawbacks of the metal matrices, such as low thermal conductivity and mechanical performance, can be compensated by doping carbon nanomaterials. Navidfar *et al.* [139] synthesized CQDs and nitrogen-enriched CQDs (N: CQD) using domestic microwave ovens. They applied these to enhance the interface bonding between carbon nanofillers and metal matrices. Their findings showed that the

24 — Yuting Xie et al. DE GRUYTER

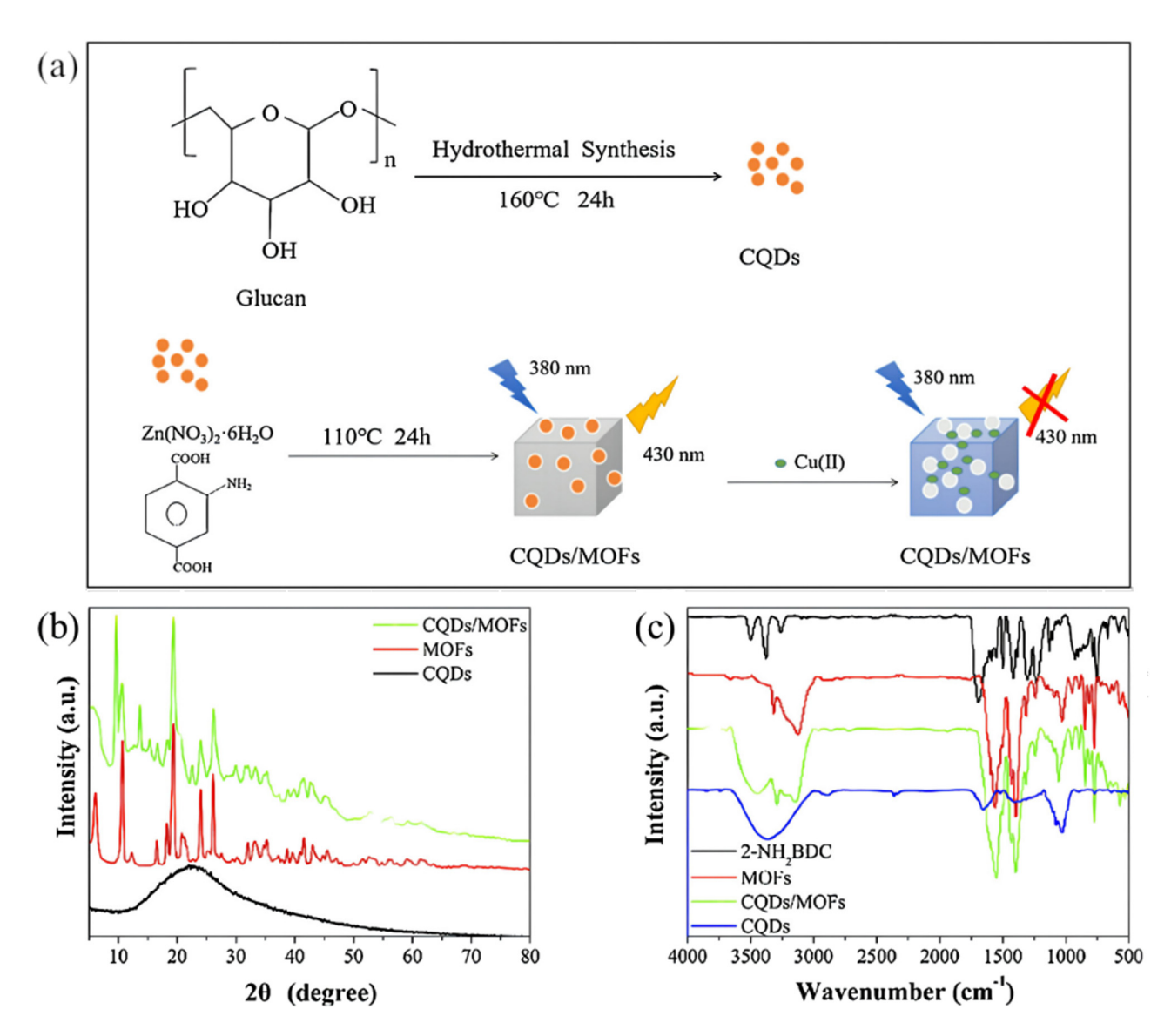


Figure 24: (a) Synthetic route for CQDs/MOFs and Cu(II) induction turn-off sensor based on the CQDs/MOFs, (b) XRD patterns, and (c) FT-IR patterns [127].

combination of CQD with graphene and CNT significantly enhanced the dispersibility of the carbon material in metal matrix, resulting in better mechanical performance and thermal stability of the composite. However, due to the different preparation processes of the composite materials, the dispersion degree of carbon nanostructures in the metal matrices is different, leading to the generation of different degrees of interface between carbon and metal phases, which also results in different strengthening mechanisms. Latif *et al.* [140] demonstrated that, in contrast to nano-reinforcements, the use of dispersing agents and/or surface modifications is not imperative for CQDs. Furthermore, the exceptionally high surface area of CQDs affords an extensive interface for stress dissipation, thereby correlating with improved mechanical properties.

During the past more than half a century of studies on metal matrix composites reinforced with carbon nanomaterials, four main strengthening mechanisms have been proposed for carbon nanomaterials within these composites: (1) Grain refinement; (2) load transfer strengthening; (3) thermal mismatch-dislocation strengthening; and (4) Orowan reinforcement. These mechanisms are considered to occur simultaneously (Figure 26) [141].

### 4.1.1 Load transfer strengthening mechanism of CQDsreinforced metal matrix composites

It is widely considered that the load transfer mechanism is crucial in enhancing the strength of metal matrix composites

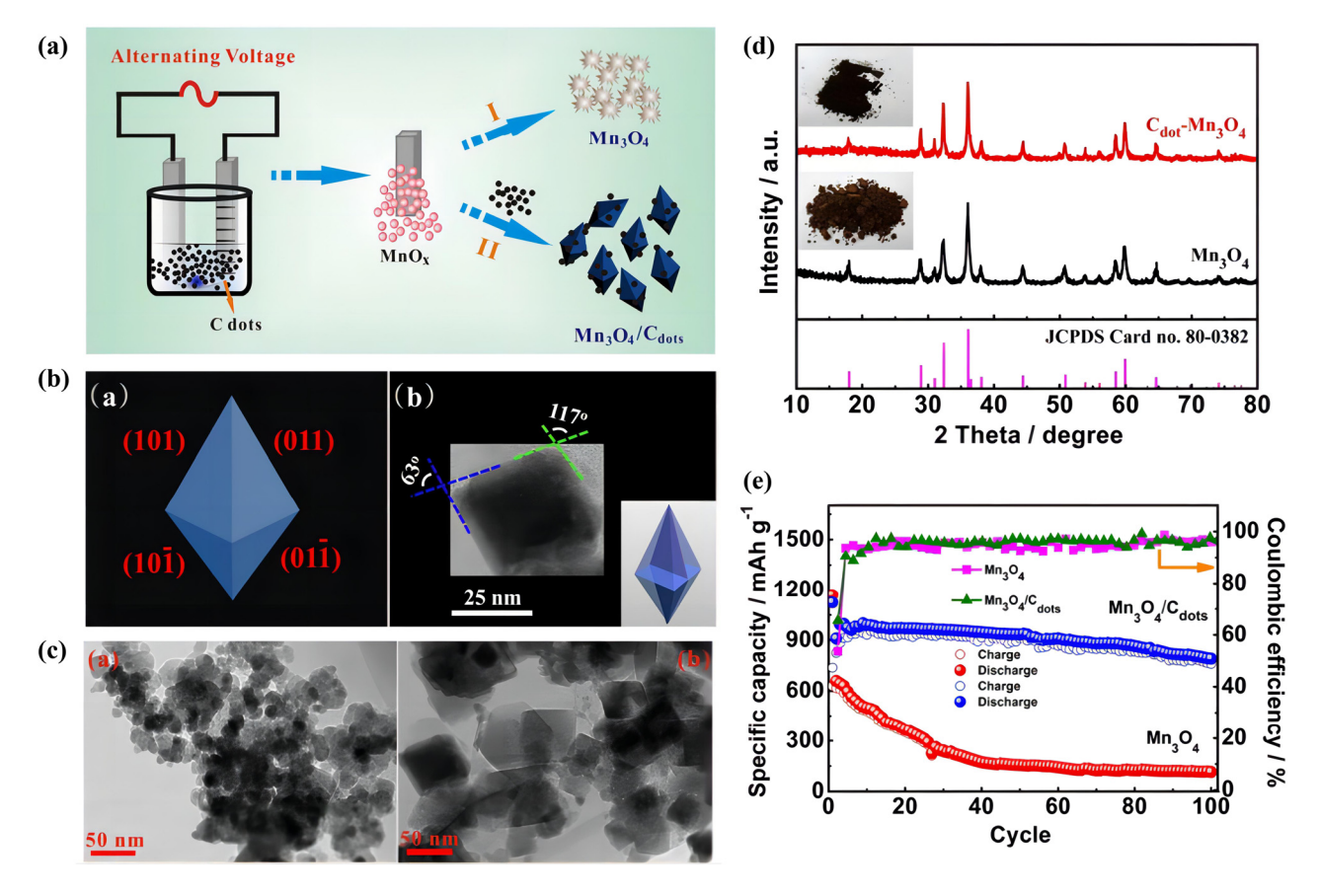


**Figure 25:** (a) Preparation of  $Mn_3O_4$  and  $Mn_3O_4/C_{dots}$  composite, (b) 3D geometrical model image of  $Mn_3O_4$  octahedron. (a) Simulation model, (b) Micrograph, (c) TEM images of  $Mn_3O_4$  and  $Mn_3O_4/C$ dots composite. (a) TEM images of  $Mn_3O_4$ . (b) TEM images of  $Mn_3O_4/C$ dots composite. (d) XRD patterns of pure  $Mn_3O_4$  and  $Mn_3O_4/C_{dots}$  composite, and (e) cycling performances and Coulombic efficiencies of the pure  $Mn_3O_4$  and  $Mn_3O_4/C_{dots}$  composite at a current density of 100 mA  $g^{-1}$  [138].

reinforced with carbon nanomaterials [142]. The basis theory is that when the metal matrix composite is loaded, it produces a relative displacement to the carbon nanomaterial along the stress direction, thus transferring the shear stress from metal matrix to reinforcement component through the interface [143]. Huang *et al.* [72] found that the interfacial bonding strength between metal matrix and reinforcing agent affects the efficiency of load transfer, and then further influences the composite material's structural integrity and conductivity (Figure 27).

Additionally, the load transfer efficiency is also influenced by some other parameters, such as the structure type and dispersion degree of reinforcement component, as well as the interaction area between the metal matrix and reinforcement component [144,145]. Based on the shear lag model introduced by Kelly *et al.* [145], the increment in tensile strength in load transfer of discontinuous fiber reinforced metal matrix composites could be determined with the following equations:

$$\Delta \sigma_{LT} = V_f \sigma_f \left[ 1 - \frac{l_c}{2l} \right] + \sigma_m (1 - V_f) - \sigma_m, \quad (l \ge l_c), \quad (3)$$

$$\Delta \sigma_{LT} = V_f \left( \frac{\tau_y}{d} \right) l + \sigma_m (1 - V_f) - \sigma_m, \quad (l \le l_c), \quad (4)$$

$$l_{\rm c} = d \left[ \frac{\sigma_{\rm f}}{2\tau_{\rm y}} \right] \left[ \tau_{\rm y} \approx \frac{\sigma_{\rm m}}{2} \right],$$
 (5)

where  $\Delta\sigma_{\rm LT}$  represents the increment in tensile strength of the composite under load transfer strengthening, and  $V_{\rm f}$  represents the volume fraction of reinforcement agent in metal matrix.  $\sigma_{\rm f}$  and  $l_{\rm c}$  represent the tensile strength and critical length of reinforcement agent, respectively. d and l represent the diameter and length of reinforcement agent, respectively.  $\sigma_{\rm m}$  represents the tensile strength of metal matrix, and  $\tau_{\rm y}$  represents the YS of metal matrix. By generating a strong interface bonding, the metal matrix composite can transfer most of the stress to the reinforcement agent when it is subjected to external loading, thus

26 — Yuting Xie et al. DE GRUYTER

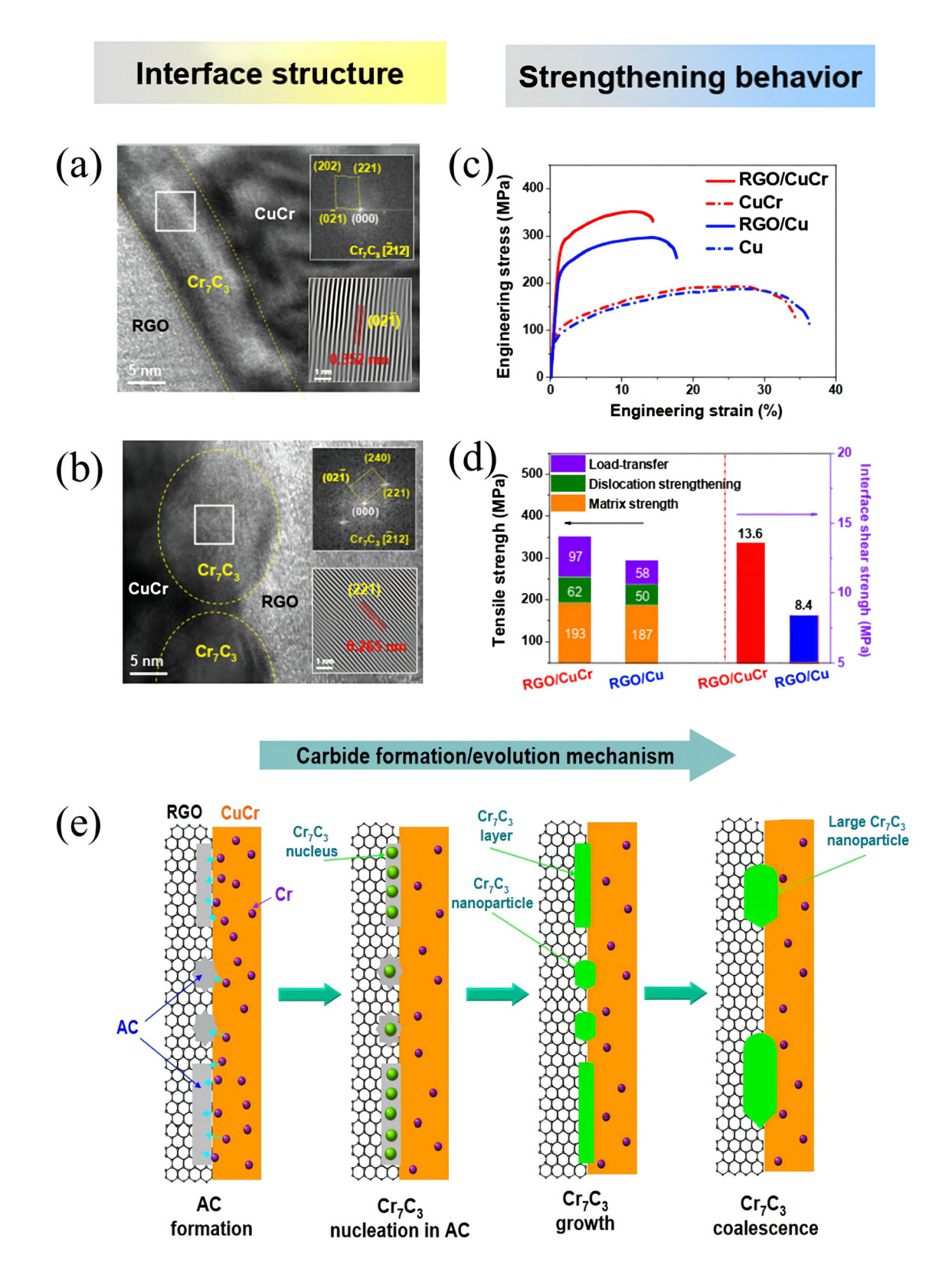


**Figure 26:** (a) and (b) HRTEM images of RGO-CuCr interface, (c) engineering stress–strain curves of RGO/Cu and RGO/CuCr composites with unreinforced Cu and CuCr, (d) reinforcement contributions (left part) and interface shear strength (right part) of RGO/CuCr and RGO/Cu composites, and (e) the possible carbide formation/evolution mechanism in RGO/CuCr composite [13].

significantly improving the distribution of shear stress and the tensile strength of the composite material.

### 4.1.2 Thermal mismatch strengthening mechanism of CQDs-reinforced metal matrix composites

Thermal mismatch strengthening mechanism of the metal matrix composites is related to the high-density dislocation caused by the significant disparity in thermal expansion coefficients between the metal matrix and reinforcement agent [146]. In CQDs-reinforced copper matrix composite, the metal matrix has higher thermal expansion coefficient than the carbon material. During heat treatment and plastic deformation, the large SSA of CQDs will result in the formation of dislocation accumulation near the interface, thus hindering the movement of grain boundaries. In particular, with the continuous increase in the sintering

temperature, the mismatch stress in the interface area and the dislocation also increases, contributing to the enhancement of the mechanical properties of CQDs/metal matrix composites. There are many methods to calculate the tensile strength of the carbon material reinforced metal matrix composites under thermal mismatch strengthening. For example, Elomari *et al.* [147] calculated the increment in tensile strength by using the following modified model:

$$\Delta \sigma_{\rm TM} = aGb \sqrt{\frac{12V_{\rm f}\Delta CTE\Delta T}{bd_{\rm p}}}, \qquad (6)$$

where  $\Delta\sigma_{\rm TM}$  represents the increment in tensile strength of the composite under thermal mismatch strengthening, a is a constant, G and b represent the shear modulus and the Bernoulli vector of metal matrix, respectively.  $V_{\rm f}$  represents the volume fraction of reinforcement agent in metal matrix,  $\Delta$ CTE indicates the variation in thermal expansion coefficients between metal matrix and reinforcement agent,

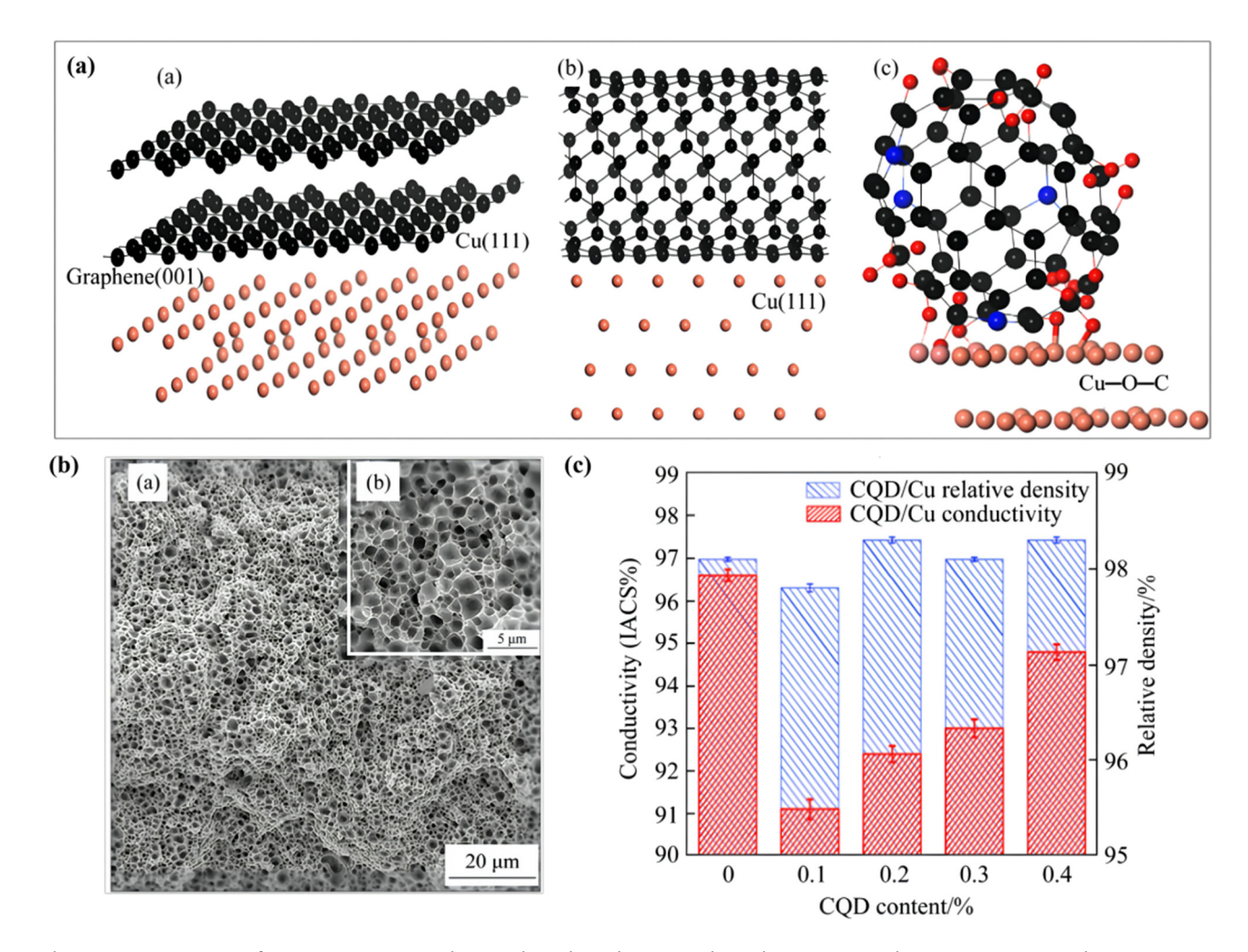


**Figure 27:** (a) Atomic interface structures, (a) Graphene and Cu; (b) Carbon nanotube and Cu; (c) CQD and Cu grain (Cu, O, N and C atoms are represented by pink, red, blue and black balls, respectively). (b) fracture morphology of CQD/Cu composites under tensile test, (a) The range is 20 micron. (b) the range is 5 micron. (c) relative density and electrical conductivity of Cu and CQD/Cu composites [72].

 $\Delta T$  represents the maximum difference in temperature during thermal processing, and  $d_{\rm p}$  represents the diameter of the reinforcement agent.

Orowan strengthening mechanism of CQDs-reinforced metal matrix composites is also important. Orowan strengthening means that when the dislocation encounters the obstruction and accumulation of the reinforcement agent, it moves forward by bypassing the reinforcement agent and forms a dislocation ring around the reinforcement agent, resulting in an elevation of lattice distortion energy and resistance to dislocations, improving the strength of metal matrix composites [148]. According to Orowan-Ashby equation [149] as shown below, the increment in tensile strength of the carbon nanomaterials reinforced metal matrix composites under Orowan strengthening can be predicted.

$$\Delta \sigma_{\text{Orowan}} = \frac{0.13Gb}{\lambda} \text{In} \left( \frac{d_{\text{p}}}{2b} \right),$$
 (7)

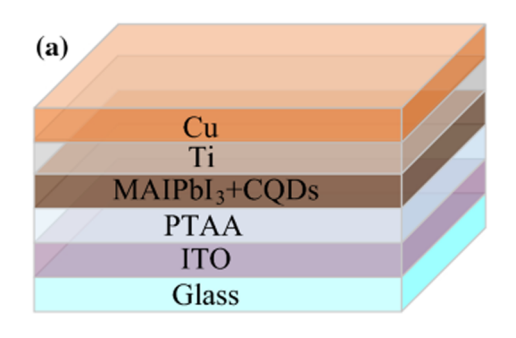
where  $\Delta\sigma_{\rm Orowan}$  represents the increment in tensile strength of the composite under Orowan strengthening, G and b represent the shear modulus and the Bernoulli vector of metal matrix, respectively.  $\lambda$  represents the effective plane spacing between reinforcements ( $\lambda = d_p \pi/2f_v$ ),  $d_p$  represents the reinforcement component diameter. The Orowan model is more suitable to explain the strengthening mechanism of reinforced composites with smaller size.

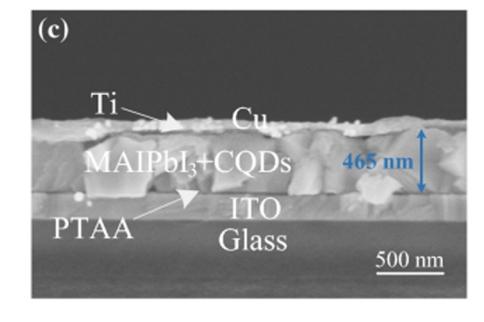
Wen et al. [150] strengthened high-quality  $CH_3NH_3PbI_3$  (MAPbI<sub>3</sub>) films with CQDs (Figure 28) and found that CQDs

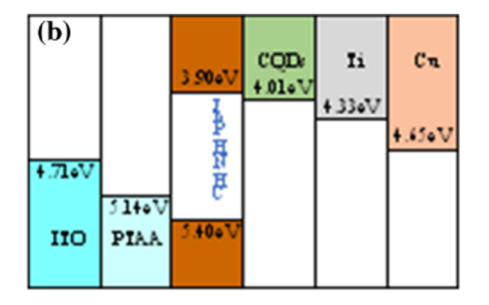
with a proper concentration of 0.04 mg mL<sup>-1</sup> passivated the imperfections in the crystal structure of MAPbI<sub>3</sub> films through Orowan strengthening mechanism, which could augment the size of the grains and crystallinity, and decrease the presence of grain boundaries. Guan et al. [151] used CQDs as dopants to prepare metal composite materials CsPbBr<sub>3</sub>@CQDs, and explored the strengthening mechanism of the metal matrix composite with CODs. The results reveal that the introduction of CQDs could passivate the surface lattice defects on CsPbBr<sub>3</sub> based on the Orowan strengthening mechanism, which enhances the tensile strength of CsPbBr<sub>3</sub>@CQDs, resulting in good water stability and photoinduced charge transfer performance of the composite. Huang et al. [72] investigated the strengthening effects of CQD nanomaterial reinforcement CQD/Cu composite. The results show that the tensile strength and YSs of CQD/Cu exceed those observed in pure copper samples. Moreover, the tensile strength of the CQD/Cu composite gradually increases with the CQD content. However, a consequent reduction in elongation was observed for the material.

### 4.1.3 Fine grain strengthening mechanism of CQDsreinforced metal matrix composites

Fine grain strengthening refers to reinforcing the metal matrix composites by refining the grain size within the composites [152]. In the reinforced composite systems,







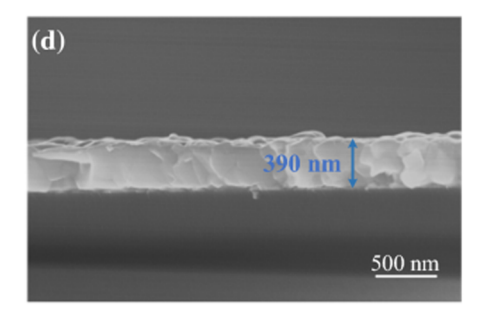


Figure 28: (a) The PSC, (b) energy band diagram, (c) cross-sectional SEM image of the PSC (0.04 mg mL<sup>-1</sup> CQDs additive), and (d) cross-sectional SEM of MAPbI3 film [150].

when carbon nanomaterials are added, due to the pinning effect, the carbon nanomaterials reinforced phase becomes the substrate of metal heterogeneous nucleation, thus improving its nucleation rate, hindering the movement of grain boundaries, and inhibiting the growth of grains [153] (Figure 29). The increase in grain nucleation rate can enhance the quantity of grain boundaries, thus suppressing the movement of dislocations when deformation occurs, causing the formation of dislocation pile-up at the grain boundaries, thus achieving the effect of fine grain strengthening. The evolution from plastic deformation to ductile fracture is a process from crack generation to crack propagation when the composite material is subjected to external force. Finer grain size of metal matrix composite leads to higher concentrated stress and energy required for crack generation and propagation, i.e., the larger tensile strength of the metal matrix composite. He et al. [154] added N-CQDs to MoS2 nanofluids and investigated their tribological and mechanical performances. The analysis results show that the strengthening effect of CQDs contributes to the formation of ultrafine crystalline NPs in the metal matrix composite. Besides, the interaction of the steel surface with S atoms in MoS<sub>2</sub> and the organic functional groups on N-CQDs surface enhances the strength and stability of the composite. This further protects the metal surface from friction and wearing. Yin et al. [155] compared, under the same conditions, the

CQDs@HG and HG's compressive stresses and they were found to be 1.65 and 1.17 MPa (under 90% strain). The reason why CQDs@HG's compressive stresses is higher is that hydrogen bonds between the CQDs and hydrogel matrix absorb some of the compressive energy when they preferentially break.

### 4.2 Electrical properties

CQDs with different surface passivation structures could efficiently induce crystal growth. They could act as a "design additive" to change the morphologies and surface structures of the composites [156]. Recently, many studies have underscored the utility of CQDs as a conductive additive in the realm of electrochemical energy storage. As the electrode material of supercapacitors, CQD-modified RuO<sub>2</sub> shows an elevated specific capacitance of 460 F g<sup>-1</sup> at current density of 50 A g<sup>-1</sup> [157]. As the anode material of lithium-ion batteries, Nb<sub>2</sub>O<sub>5</sub>/CQDs nanocomposite exhibits a capacity of 385 mA h g<sup>-1</sup> after 100 cycles at a current density of 0.1 A g<sup>-1</sup>. It is a promising topic to develop novel composite electrodes for sodium ion batteries (SIB) by combining active materials and CQDs to achieve distinctive structures and properties. Liu *et al.* [158] synthesized

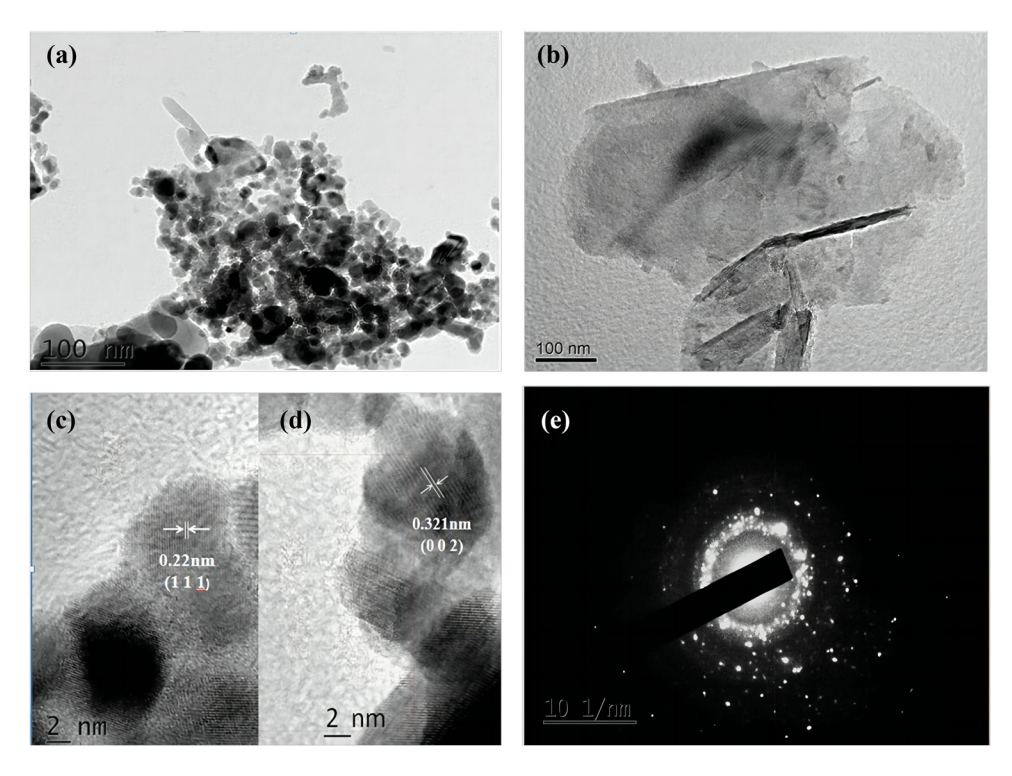


Figure 29: Characterization of the CQDs@NiCoP composite. (a) and (b) Low magnification TEM images. (c) and (d) High magnification TEM images. (e) SAED pattern of CQDs@NiCoP [153].

Sb@CQDs composite material using a simple one-step reduction method at 25°C and used it for high performance SIB. The inclusion of residual CQDs within the Sb@CQDs composite was found to augment the electronic conductivity of the material. Thanks to the CQD modification, the composite material showcased an impressive specific capacity of 635 and 334 mA h g $^{-1}$  at current densities of 0.1 and 2 A g $^{-1}$ , respectively.

As a new type of carbon nanomaterials with ultra-high conductivity in electrochemical reactions, CQDs have demonstrated significant potential for application in electrocatalysis with the purpose of rapid electron transfer [159]. Zhao et al. [160] constructed CQDs/SnO<sub>2</sub>-Co<sub>3</sub>O<sub>4</sub> nanocomposites via a simple hydrothermal process. It was observed that CQDs improved the material conductivity, and promoted the electron transfer between the catalyst active sites and electronic surfaces, resulting in a significantly enhanced electrocatalytic performance of the composite material for water oxidation. Yang et al. [161] synthesized Co and Fe co-doped CQD (CoFeCQD) using a simple one-pot hydrothermal approach and found that CODs substantially enhanced material's conductivity and facilitated electron transfer in the electrocatalytic reaction. This led to an obvious enhancement in both the performance and durability of the composite electrocatalyst for OER.

In addition, it has also been proven that CQDs can improve the stability of metal matrix composite catalysts due to their high degree of surface functionality and excellent chemical stability in a variety of media. In composites of CQDs and metal or metal oxide, CQDs can act as barriers to inhibit metal or metal oxide nanostructures from aggregation, thus dramatically improving the composite's catalytic activity. Conversely, the electrostatic stability of CQDs offers the material high stability in aqueous solutions. Besides, the strong electrostatic interaction between CODs and metal substrate in the composite also significantly improves the material's stability. For example, Tang et al. [162] synthesized CQD/NiFe-LDH composite materials and studied their electrochemical properties. The robust electrostatic interaction among CQDs, NiFe-LDH, and the resulting C-O-Ni/Fe bonds contribute greatly to enhancing the electrochemical stability of CQD/NiFe-LDH composites for OER. Therefore, CQDs play a crucial role in improving the electrocatalytic properties of metal matrix composites. Their effects include enhancing conductivity, varying morphological characteristic and crystal phase, optimizing electronic structure, providing new active and defect sites, as well as improving stability. Han et al. [163] prepared CQDs using Xylan and incorporated them into Ag NPs and rGO to produce composite materials. High sensitivity for detection of DA was achieved by using this composite modified GCE,

which could be explained by the high catalytic activity and conductivity of the modified electrode.

The CQDs prepared by Huang et al. [164] via sucrose carbonization was mixed with Cu<sub>2</sub>O NPs under ultrasonic treatment in the presence of Nafion (as adhesive) to prepare the strengthened metal matrix composite CQD@Cu<sub>2</sub>O. Test results show that the GCE modified by CQD@Cu2O has good sensing performance, which is mainly due to the high conductivity of Cu<sub>2</sub>O NPs and electrostatic attraction between CQDs (and Nafion) and DA at physiological pH. Elugoke et al. [96] compared the electrode surface areas and electrical properties of different GCEs with and without CuO and CQD. The results showed that the electrode surface areas of bare GCE, GCE/CuO, GCE/CQD, and GCE/CQD/CuO were 0.25, 0.10, 0.07, and 0.54 cm<sup>2</sup>, respectively. The current response to oxidation in the nanocomposite modified GCE/ CQD/CuO electrode was also significantly higher than that of other electrodes. The reason might be the larger value of effective surface area in GCE/CQD/CuO, as well as other possible factors, e.g., the synergistic interaction of CuO and CQD in the composite. Moreover, in comparison with other electrodes, the redox reaction on the GCE/CQD/CuO electrode occurs at lower potential (Figure 30).

Moreover, Chen *et al.* [165] synthesized N-CQDs modified  $SnO_2$  NPs ( $SnO_2$ /NCQDs) using simple hydrothermal process. The introduction of N-CQDs can improve the efficiency of electron and hole separation, thereby accelerating electron transfer. Tamal *et al.* [166] prepared metal matrix composites strengthened with  $Fe_3O_4$  NPs and CQDs (CQD@Fe\_3O\_4 NPs) by wet chemical coprecipitation method. The insertion of CQDs into the surface of  $Fe_3O_4$  NPs leads to change in interface properties and reduction in electron scattering.

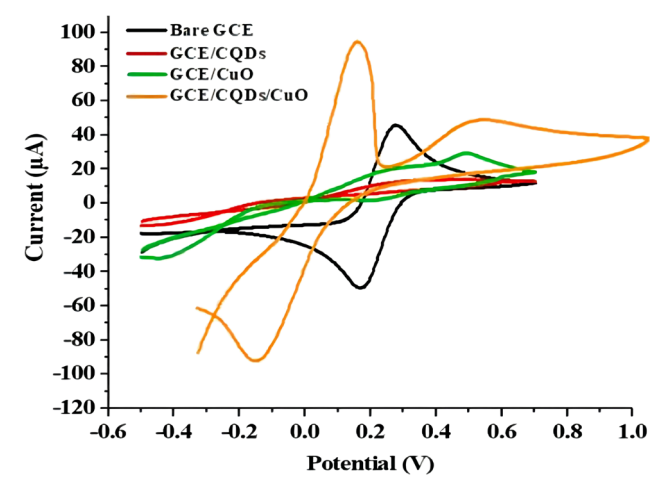


**Figure 30:** Cyclic voltammogram of bare GCE, GCE/CQDs, GCE/CuO, and GCE/CQDs/CuO in 10 mM [Fe(CN)<sub>6</sub>] $^{3-/4-}$  redox probe in PBS (pH 7.0) at a scan rate of 25 mV s<sup>-1</sup> [96].

In summary, the electrical characteristics of metal matrix composites reinforced with CODs are primarily influenced by their electronic structure, geometric morphology, and conductivity. Based on the diminutive size, extensive surface area, elevated conductivity, and easy access to surface functions of CQDs, their impact on the electrical properties of CQD-based composites can be summarized to the following aspects: (1) CQDs could effectively improve the conductivity and electron transfer rate of metal matrix composites; (2) CQDs can efficiently modify the morphological feature and crystal structure, including generating additional surface active sites and improving the intrinsic activities of the sites; (3) The charge distribution and electronic structure of CQDs-based composites can be adjusted to promote the adsorption/desorption of the intermediates, thereby significantly improving the electrocatalytic properties; (4) The large surface areas of CQDs can offer a big amount of electrocatalytically active edges and defects for reactions; (5) The strong electrostatic interaction between CQDs and catalytic materials could also improve the electrochemical stability of metal matrix composites.

### 4.3 Thermal properties

The metal matrix composites strengthened by CQDs also show clear changes in their thermal properties, mainly due to two reasons. On the one hand, CQDs enhance the bonding interface of the composite, and the strong bonding interface limits the formation of electronic potential barrier, electronic scattering and phonon scattering, which improves the thermal properties of the composite [167]. On the other hand, CQDs start to burn at 510°C, which destroys their strengthening effect on composites. Chen et al. [165] synthesized SnO<sub>2</sub> and SnO<sub>2</sub>/NCQDs composites and compared their thermal properties. It can be seen from the TGA curve (Figure 31) that SnO<sub>2</sub>/NCQDs has a higher weight loss than SnO2 at a temperature from 100 to 600°C, mainly due to the surface dihydroxylation and partial combustion of NCQDs. These results show that the introduction of NCQDs can enhance the capability of SnO<sub>2</sub> for adsorbing surface hydroxyl groups.

Liu *et al.* [158] explored the impact of synthesis temperature on the structure of Sb@CQDs composite. The temperature was raised from ambient temperature to 800°C at a rate of 10°C/min during the composite synthesis process. The TGA curve in Figure 32b shows that the weight of the composite increases at temperatures of around 318.6 and  $568.2^{\circ}$ C, which might be related to the oxidation of Sb to Sb<sub>2</sub>O<sub>3</sub> and the subsequent further oxidation to Sb<sub>2</sub>O<sub>4</sub>,

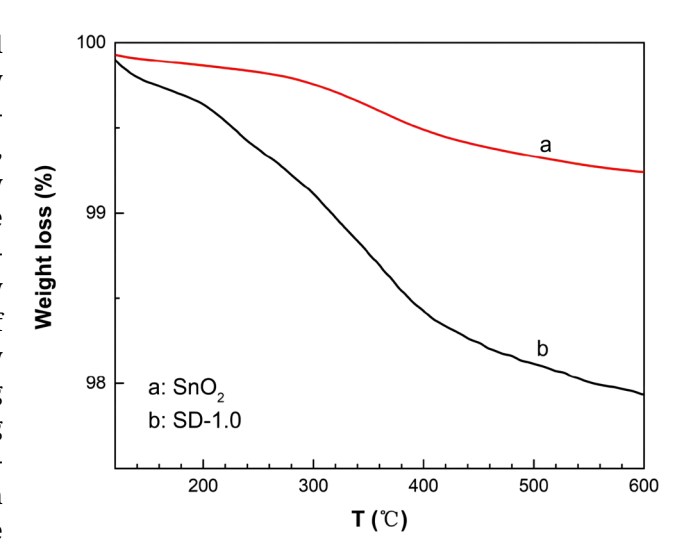


Figure 31: TGA curves of SnO<sub>2</sub> and SnO<sub>2</sub>/NCQDs composites [165].

respectively. The exothermic peak and weight reduction at 513.2°C can be attributed to the combustion of CQDs. Drawing from this reaction mechanism, it can be induced that Sb@CQDs-H has a carbon content of 12.54 wt%.

Jing *et al.* [138] analyzed the thermal properties of  $\rm Mn_3O_4/C_{dots}$  composites by TGA, and found that CQDs could strongly influence the thermal stability of the composite. The CQDs started to burn at ca. 510°C, leading to an unstable status of the composite material. Besides, a CQD content of 13.8% in the  $\rm Mn_3O_4/C_{dots}$  composite was detected.

### **5** Prospect

By virtue of the superior mechanical, electrical, thermal, and friction properties of CQDs, the combination of CQDs with metal matrix materials has improved the performances of metal matrix materials to some extent, pointing out a new pathway for exploring novel material systems with ultra-high performance or strong comprehensive performance.

It is meaningful to mention that the enhancement of strategies for high-purity, high-yield, and large-scale production of CQDs, along with the comprehensive investigation into their mechanisms of action in various emerging engineering applications, will significantly propel the transition of CNTs from fundamental research to industrial applications. Zhu *et al.* [168] introduced a magnetic hyperthermia method for producing fluorescent CQDs with up to 60% yield, showcasing a non-contact approach that enhances temperature stability and safety. In biomedical fields, CQDs are exploited for drug delivery, tissue engineering, and cellular

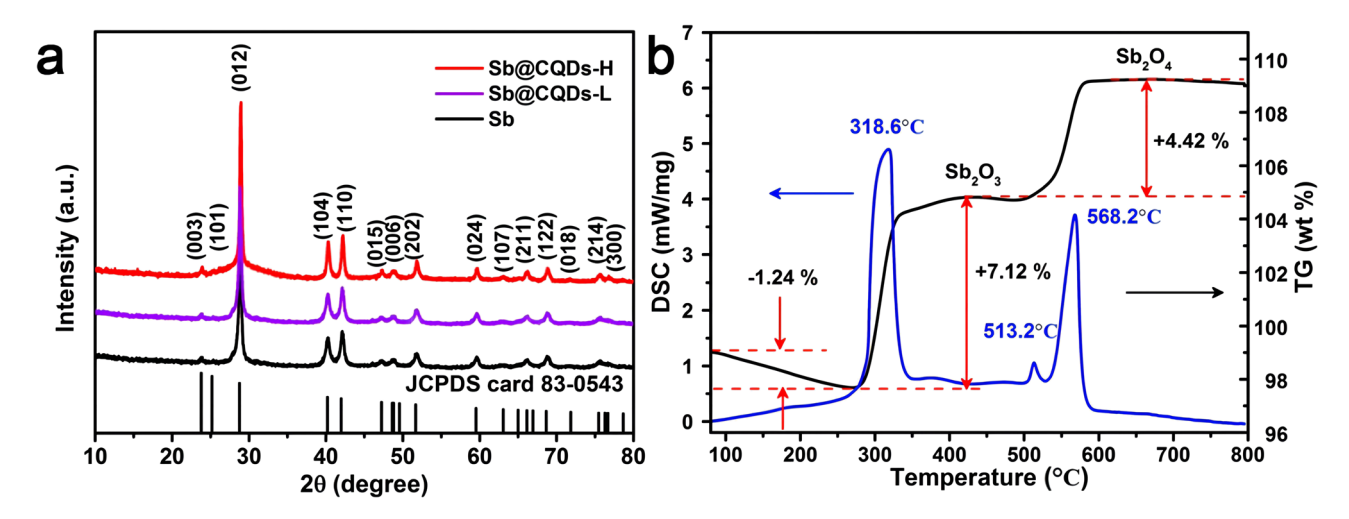


Figure 32: (a) XRD patterns of Sb@CQDs-H, Sb@CQDs-L, and Sb. (b) TGA and DSC curves of Sb@CQDs-H in air [158].

imaging due to their small size and biocompatibility, improving treatment efficacy and reducing side effects [169]. Research by Mancini *et al.* [170] demonstrated the use of CQDs derived from food industry by-products for luminescent cellular probes, while Deepika *et al.* [171] highlighted their application in creating innovative, biodegradable food packaging materials with enhanced properties.

Further, CQDs find applications in optoelectronics, water treatment, and energy sectors by improving electrochemical performance and facilitating the development of efficient devices. Franco *et al.* [172] underscored CQDs' potential as a non-toxic tracer in the oil industry, offering advantages over traditional tracers in field trials. Palanimuthu *et al.* [173] utilized CQDs synthesized from spirulina for effective photocatalytic degradation of pollutants under sunlight, and Berdimurodov *et al.* [174] explored their use as corrosion inhibitors in the oil and gas industries.

In display technology, CQDs are crucial for developing LED displays and televisions, with Urushihara *et al.* [175] discovering electroluminescent properties in CQDs synthesized from fenugreek seeds, marking significant strides in LED device manufacturing. The ongoing development of new technologies for the rapid, cost-effective production of CQDs holds substantial importance for their widespread industrial application.

However, by reviewing the research progress of CQDs in metal matrix composites, it is found that this material system is still facing issues such as inadequate dispersion of CQDs and weak CQD/metal interface bonding. The possible mechanisms for these issues and the effects of CQDs in the composite materials are described as follows. First, the surface of CQDs is enriched with a substantial quantity of organic functional groups, *e.g.*, hydroxyl, amino, carboxyl, and so on, which could efficiently enhance the wettability

between metal matrix and CQDs. However, this improvement effect derived from CQDs is very limited due to the small proportion of sp<sup>2</sup> and sp<sup>3</sup> in CODs as well as the low content of CQDs in the composite. Therefore, the dependence of the composite on the interface can be improved by increasing the load and electron transfer efficiency of the composite, thus improving the dispersion and interface bonding ability of the composite. Second, due to the reactive inertia between carbon and metal, it is difficult to directly generate interfacial carbides at the carbon-metal interface in the composite, resulting in poor wettability between CQDs and metal matrix. The next research action should focus on the combination of CQDs with suitable second phase elements to effectively solve the above problems. Composites prepared by methods of matrix alloying with improved interface bonding and optimized mechanical property have been reported, e.g., MWCNT/CuCr [176], carbon fiber/CuCr [177], and carbon nanofiber/CuTi (Zr) [178]. On the other hand, the current studies on CQDs-modified metal matrix composites focus mainly on the performances of the materials for electrochemical sensors and photocatalysis applications, while the work related to theoretical analysis and mechanism investigation are very limited.

CQDs-reinforced metal matrix composites show great potential for application from the perspective of their electrical properties, especially the electrocatalytic properties. However, to get more insight into the effects of CQDs on the electrocatalytic properties and to establish theoretical basis for designing novel electrocatalysts, several issues and challenges need to be overcome. First, more effective techniques for characterizing the electronic structures of CQDs-modified metal matrix composites are required. Catalysts with modified electronic structures can generally promote electron transfer and adsorption/desorption of reaction

intermediates, thus improving the electrocatalytic properties. However, the catalyst's electronic configuration during reaction might be different from that during characterization. Therefore, sophisticated characterization methods, such as utilizing synchrotron radiation XAS and so on, are needed to deeply understand the electronic structure of CQDs-reinforced metal matrix composites. Second, during the preparation of CODs-modified metal matrix composites, the organic groups at CQD surface provide active sites for coordination with metal ions. Nevertheless, information on the coordination between the CODs and the metal ions are currently very limited due to the lack of effective characterization techniques. Therefore, to reveal detailed reaction processes and provide theoretical guidance for fabricating CQDs-based composites with improved electrical properties, more advanced analysis methods are required, for example, in situ FTIR, in situ EXAS, in situ Raman spectroscopy, and synchrotron radiation. Both the metallic compounds and the CQDs could be involved in the electrocatalytic reactions as active centers. Determination of the role of different active sites in the reactions and the dominant electrical properties of the composite materials has important guiding significance for design of more effective electrocatalysts.

Introduction of numerical simulation, ML, and artificial intelligence (AI) in the design of metal matrix composites will be an important development direction to theoretically solve the problems of weak interface bonding, poor mechanical properties, and unstable electrical properties [179–181]. Although the structure-performance dependence of metal matrix composites is not linear, prediction heuristics (such as ligand field theory) can provide a basis for improving the performance of metal matrix composites, and prove that the structure-property correlation is a task suitable for ML. While it is difficult to predict the comprehensive properties of the metal matrix composites using first principles and physical based models (such as density functional theory [DFT]), building predictive artificial neural network (ANN) models to predict the properties of the metal matrix composites, such as spin splitting energy, redox potential, and metal bond length, will be an important research subject. Once a suitable numerical simulation model is established, it can be extended to tasks such as predicting computational results, catalytic activity, or gas absorption in MOFs. Currently, there is a lack of suitable characterization methods for the electronic structure of the interface in metal matrix composites, and it is currently not possible to directly observe the vast space of the interface. However, computational chemistry can easily traverse this space using effective methods (e.g., SQM and MM), and more rigorous first principles (e.g., DFT and wave function theory) can conduct accurate analysis of the chemical properties of metal matrix materials. The reason is partly that the direct mapping between structure and functionality paves the way for impressive ML model performance.

In addition, AI can be used not only to predict the structures and properties of composite materials, but also to analyze all data related to the overall safety of CQDs. ML algorithms can utilize all known data related to different components, properties, and behaviors of metal matrix composites (and any materials associated therewith) to predict the characteristics of composite materials. By accessing historical data and analyzing metal matrix composites of current interest. AI algorithms can execute highly accurate predictions that can be used in conjunction with physical characterization results. This is typically accomplished by comparing structural similarity to composite materials with known properties. Having all the data related to all the different chemical characteristics available is almost impossible for humans to accomplish, but AI algorithms can access (and understand) the data by inferring from scientific literature. AI can then directly predict the characteristics of CQDs and metal matrix composites of interest based on their structure and physicochemical properties.

### 6 Conclusion

Incorporation of CQDs with excellent properties into metal matrix materials can comprehensively improve the performance of the materials, which is a key to progress of this composite material to meet the requirements of mechanical and physical properties. Previous studies indicate the formation of an effective mechanical lock between CQDs and Cu, which improves the performance of the composite material. The reinforcement of metal matrix composites by CQDs is mainly reflected in three aspects, i.e., mechanical property, electrical conductivity, and thermal conductivity. Until now, many research works have been conducted on the CQDs-reinforced copper matrix composites, but there still remains an obstacle in the practical application of this material. The focus of the future studies in this area should be placed on the subsequent aspects: (1) Mechanisms of the interfacial bonding between CQDs and Cu matrices; (2) further optimized material preparation methods with processes that are highly efficient, cost-effective, and environmentally friendly; (3) integration of the research area with other subjects such as numerical simulation, ML, and AI.

It is worth mentioning that numerical simulations such as ANN models can be used to predict the performance of metal matrix composites based on their structure and physicochemical properties. AI can directly select the appropriate metal matrix composites with the required mechanical, electrical, and thermal properties for different practical applications. The future work should be targeted at development of CQDs-reinforced copper matrix composites meeting both the performance and environmental requirements of various fields to promote the large-scale application of the promising material.

**Funding information:** This work was supported by Key Laboratory of Infrared Imaging Materials and Detectors, Shanghai Institute of Technical Physics, Chinese Academy of Sciences (No. IIMDKFJJ-21-10) and China Postdoctoral Science Foundation (No. 2018T110993).

Author contributions: Investigation: Yuting Xie, Junyi Hu, Yuxin Hu, and Xiaosong Jiang. Writing — original draft preparation: Yuting Xie, Junyi Hu, and Yuxin Hu. Writing — review and editing: Yuting Xie, Junyi Hu, Yuxin Hu, and Xiaosong Jiang. Project administration: Xiaosong Jiang. All authors have accepted responsibility for the entire content of this manuscript and approved its submission.

**Conflict of interest:** The authors state no conflict of interest.

### References

- [1] Zhang H, Huang H, Ming H, Li H, Zhang L, Liu Y, et al. Carbon quantum dots/Ag<sub>3</sub>PO<sub>4</sub> complex photocatalysts with enhanced photocatalytic activity and stability under visible light. J Mater Chem C. 2012;22(21):10501–6.
- [2] Malavika JP, Shobana C, Ragupathi M, Kumar P, Lee YS, Govarthanan M, et al. A sustainable green synthesis of functionalized biocompatible carbon quantum dots from Aloe barbadensis Miller and its multifunctional applications. Environ Res. 2021;200:111414.
- [3] Mondal S, Das SR, Sahoo L, Dutta S, Gautam UK. Light-induced hypoxia in carbon quantum dots and ultrahigh photocatalytic efficiency. J Am Chem Soc. 2022;144(6):2580–9.
- [4] Xie C, Nie B, Zeng L, Liang FX, Wang MZ, Luo L, et al. Core-shell heterojunction of silicon nanowire arrays and carbon quantum dots for photovoltaic devices and self-driven photodetectors. ACS Nano. 2014;8(4):4015–22.
- [5] Zhu Z, Ma J, Wang Z, Mu C, Fan Z, Du L, et al. Efficiency enhancement of perovskite solar cells through fast electron extraction: the role of graphene quantum dots. J Am Chem Soc. 2014;136(10):3760–3.
- [6] Li X, Liu Y, Song X, Wang H, Gu H, Zeng H. Intercrossed carbon nanorings with pure surface states as low-cost and environment-friendly phosphors for white-light-emitting diodes. Angew Chem. 2015;127(6):1779–84.
- [7] Yuan F, Yuan T, Sui L, Wang Z, Xi Z, Li Y, et al. Engineering triangular carbon quantum dots with unprecedented narrow bandwidth emission for multicolored LEDs. Nat Commun. 2018;9(1):2249.

- [8] Kim HH, Lee YJ, Park C, Yu S, Won SO, Seo WS, et al. Bottom-up synthesis of carbon quantum dots with high performance photoand electroluminescence. Part Part Syst Charact. 2018;35(7):1800080.
- [9] Dager A, Baliyan A, Kurosu S, Maekawa T, Tachibana M. Ultrafast synthesis of carbon quantum dots from fenugreek seeds using microwave plasma enhanced decomposition: Application of C-QDs to grow fluorescent protein crystals. Sci Rep. 2020;10(1):1–15.
- [10] Niyogi S, Hamon MA, Perea DE, Kang CB, Zhao B, Pal SK, et al. Ultrasonic dispersions of single-walled carbon nanotubes. J Phys Chem B. 2003;107(34):8799–804.
- [11] Rashad M, Pan F, Zhang J, Asif M. Use of high energy ball milling to study the role of graphene nanoplatelets and carbon nanotubes reinforced magnesium alloy. J Alloy Compd. 2015;646:223–32.
- [12] Nam DH, Cha SI, Lim BK, Park HM, Han DS, Hong SH. Synergistic strengthening by load transfer mechanism and grain refinement of CNT/Al-Cu composites. Carbon. 2012;50(7):2417–23.
- [13] Chu K, Wang F, Li YB, Wang XH, Huang DJ, Zhang H. Interface structure and strengthening behavior of graphene/CuCr composites. Carbon. 2018;133:127–39.
- [14] Hagiwara K, Uchida H, Suzuki Y, Hayashita T, Torigoe K, Kida T, et al. Role of alkan-1-ol solvents in the synthesis of yellow luminescent carbon quantum dots (CQDs): van der Waals forcecaused aggregation and agglomeration. RSC Adv. 2020;10(24):14396–402.
- [15] Song D, Guo H, Huang K, Zhang H, Chen J, Wang L, et al. Carboxylated carbon quantum dot-induced binary metal-organic framework nanosheet synthesis to boost the electrocatalytic performance. Mater Today. 2022;54:42–51.
- [16] Jo MH, Kim KH, Ahn HJ. P-doped carbon quantum dot graftfunctionalized amorphous WO<sub>3</sub> for stable and flexible electrochromic energy-storage devices. Chem Eng J. 2022;445:136826.
- [17] Li Y, Fan L, Shui X, Fan J, Feng X, Tao T. Boosted photocatalytic activity of LaFeO<sub>3</sub>/Ag<sub>3</sub>PO<sub>4</sub> heterojunction via carbon quantum dots: Higher conductivity, stability, and dispersivity. Colloids Surf A: Physicochem Eng Asp. 2022;652:12989.
- [18] Rani UA, Ng LY, Ng CY, Mahmoudi E. A review of carbon quantum dots and their applications in wastewater treatment. Adv Colloid Interface Sci. 2020;278:102124.
- [19] Yuan F, Xi Z, Shi X, Li Y, Li X, Wang Z, et al. Ultrastable and low-threshold random lasing from narrow-bandwidth-emission tri-angular carbon quantum dots. Adv Optical Mater. 2019;7(2):1801202.
- [20] Tian L, Wang J, Wang K, Wo H, Wang X, Zhuang W, et al. Carbon-quantum-dots-embedded  $MnO_2$  nanoflower as an efficient electrocatalyst for oxygen evolution in alkaline media. Carbon. 2018;143:457–66.
- [21] Yuan T, Meng T, He P, Shi Y, Li Y, Li X, et al. Carbon quantum dots: an emerging material for optoelectronic applications. J Mater Chem C. 2019;7(23):6820–35.
- [22] De B, Karak N. Recent progress in carbon dot–metal based nanohybrids for photochemical and electrochemical applications. J Mater Chem A. 2017;5(5):1826–59.
- [23] Sidorov AI, Lebedev VF, Kobranova AA, Nashchekin AV. Formation of carbon quantum dots and nanodiamonds in laser ablation of a carbon film. Quantum Electron. 2018;48(1):45–48.
- [24] Yan Y, Li H, Wang Q, Mao H, Kun W. Controllable ionic liquidassisted electrochemical exfoliation of carbon fibers for the green and large-scale preparation of functionalized graphene quantum

- dots endowed with multicolor emission and size tunability. J Mater Chem C. 2017;5(24):6092-100.
- An Q, Lin Q, Huang X, Zhou R, Guo X, Xu W, et al. Electrochemical [25] synthesis of carbon dots with a Stokes shift of 309 nm for sensing of Fe<sup>3+</sup> and ascorbic acid. Dye Pigment. 2021;185:108878.
- Jia J, Sun Y, Zhang Y, Liu Q, Cao J, Huang G, et al. Facile and efficient fabrication of bandgap tunable carbon quantum dots derived from anthracite and their photoluminescence properties. Front Chem. 2020;8:123.
- [27] Chao-Mujica FJ, Garcia-Hernández L, Camacho-López S, Camacho-López M, Camacho-López MA, Reyes Contreras D, et al. Carbon quantum dots by submerged arc discharge in water: Synthesis, characterization, and mechanism of formation. J Appl Phys. 2021:129(16):163301.
- Cui L, Ren X, Wang J, Sun M. Synthesis of homogeneous carbon [28] quantum dots by ultrafast dual-beam pulsed laser ablation for bioimaging. Mater Today Nano. 2020;12:100091.
- [29] Sadrolhosseini AR, Beygisangchin M, Shafie S, Rashid SA, Nezakati H. Laser ablated titanium oxide nanoparticles in carbon quantum dots solution for detection of sugar using fluorescence spectroscopy. Mater Res Express. 2021;8(10):105003.
- [30] Yu H, Li X, Zeng X, Lu Y. Preparation of carbon dots by nonfocusing pulsed laser irradiation in toluene. Chem Commun. 2016;52(4):819-22.
- [31] Liu M, Xu Y, Niu F, Gooding JJ, Liu J. Carbon quantum dots directly generated from electrochemical oxidation of graphite electrodes in alkaline alcohols and the applications for specific ferric ion detection and cell imaging. Analyst. 2016;141(9):2657-64.
- [32] Canevari TC, Nakamura M, Cincotto FH, de Melo FM, Toma HE. High performance electrochemical sensors for dopamine and epinephrine using nanocrystalline carbon quantum dots obtained under controlled chronoamperometric conditions. Electrochim Acta. 2016;209:464-70.
- Kushwaha N, Mittal J, Pandey S, Kumar R. High temperature acidic oxidation of multiwalled Carbon nanotubes and synthesis of Graphene quantum dots. Int J Nano Dimens. 2018;9(2): 191-7.
- Sha R, Jones SS, Vishnu N, Soundiraraju B, Badhulika S. A novel biomass derived carbon quantum dots for highly sensitive and selective detection of hydrazine. Electroanalysis. 2018;30(10):2228-32.
- [35] Murugan N, Prakash M, Jayakumar M, Sundaramurthy A, Sundramoorthy AK. Green synthesis of fluorescent carbon quantum dots from Eleusine coracana and their application as a fluorescence 'turn-off' sensor probe for selective detection of Cu<sup>2+</sup>. Appl Surf Sci. 2019;476:468-80.
- Ahlawat A, Dhiman TK, Solanki PR, Rana PS. Facile synthesis of [36] carbon dots via pyrolysis and their application in photocatalytic degradation of rhodamine B (RhB). Environ Sci Pollut Res. 2023;30:1-8.
- [37] Pajewska-Szmyt M, Buszewski B, Gadzała-Kopciuch R. Sulphur and nitrogen doped carbon dots synthesis by microwave assisted method as quantitative analytical nano-tool for mercury ion sensing. Mater Chem Phys. 2020;242:122484.
- [38] Başoğlu A, Ocak Ü, Gümrükçüoğlu A. Synthesis of microwaveassisted fluorescence carbon quantum dots using roastedchickpeas and its applications for sensitive and selective detection of Fe<sup>3+</sup> ions. | fluorescence. 2020;30:515–26.
- Tadesse A. Hagos M. Rama Devi D. Basavajah K. Belachew N. Fluorescent-nitrogen-doped carbon quantum dots derived from

- citrus lemon juice: green synthesis, mercury (II) ion sensing, and live cell imaging. ACS omega. 2020;5(8):3889-98.
- [40] Kang J, Kim J, Kang D. Synthesis of carbon quantum dot synthesized using spent coffee ground as a biomass exhibiting visiblelight-driven antimicrobial activity against foodborne pathogens. J Food Eng. 2024;365:111820.
- [41] Atchudan R, Edison TNJI, Shanmugam M, Perumal S, Somanathan T, Lee YR. Sustainable synthesis of carbon quantum dots from banana peel waste using hydrothermal process for in vivo bioimaging. Phys E Low Dimens Syst Nanostruct. 2020:126:114417.
- [42] da Silva Júnior AH, Macuvele DLP, Riella HG, Soares C, Padoin N. Novel carbon dots for zinc sensing from Campomanesia phaea. Mater Lett. 2021:283:128813.
- Hoan BT, Tam PD, Pham VH. Green synthesis of highly lumines-[43] cent carbon quantum dots from lemon juice. J Nanotechnol. 2019:2019:1-9.
- [44] Zhou J, Zhang Y, Ding J, Fang J, Yang J, Xie Y, et al. A more efficient method for preparing a MIP-CQDs/ZnO<sub>1-x</sub> photodegradant with highly selective adsorption and photocatalytic properties. ACS Appl Mater & Interfaces. 2024;16(2):2365-77.
- [45] Mindivan F, Goktas M. The green synthesis of carbon quantum dots (CQDs) and characterization of polycaprolactone (PCL/CQDs) films. Colloid Surf A-Physicochem Eng Asp. 2023;667:132446.
- [46] Boruah A, Saikia M, Das T, Goswamee RL, Saikia BK. Blue-emitting fluorescent carbon quantum dots from waste biomass sources and their application in fluoride ion detection in water. J Photochem Photobiol, B: Biol. 2020;209:111940.
- Hu CS, Zhu YM, Zhao XF. On-off-on nanosensors of carbon [47] quantum dots derived from coal tar pitch for the detection of Cu<sup>2+</sup>, Fe<sup>3+</sup>, and L-ascorbic acid. Spectrochim Acta Part A: Mol Biomol Spectrosc. 2020;250:119325.
- [48] Liu YM, Roy S, Sarkar S, Xu J, Zhao YF, Zhang JJ. A review of carbon dots and their composite materials for electrochemical energy technologies. Carbon Energy. 2021;3(5):795-826.
- [49] Pandey R, Ram C, Charles C. Carbon nanotubes, graphene, and carbon dots as electrochemical biosensing composites. Molecules. 2021;26(21):6674.
- [50] Shinde DB, Pillai VK. Electrochemical preparation of luminescent graphene quantum dots from multiwalled carbon nanotubes. Chemistry. 2012;18(39):12522-8.
- [51] Naghdi T, Atashi M, Golmohammadi H, Saeedi I, Alanezhad M. Carbon quantum dots originated from chitin nanofibers as a fluorescent chemoprobe for drug sensing. J Ind Eng Chem. 2017:52:162-7.
- [52] Muthusankar G, Sasikumar R, Chen SM. Electrochemical synthesis of nitrogen-doped carbon quantum dots decorated copper oxide for the sensitive and selective detection of non-steroidal anti-inflammatory drug in berries. J Colloid Interface Sci. 2018;523:191–200.
- [53] Wang X, Yang P, Feng Q, Meng T, Wei J, Xu C, Han J. Green preparation of fluorescent carbon quantum dots from cyanobacteria for biological imaging. Polymers. 2019;11(4):616.
- Tian L, Chen F, Ding H, Li XH, Li XB. The influence of inorganic [54] electrolyte on the properties of carbon quantum dots in electrochemical exfoliation. J Electroanal Chem. 2020;878:114673.
- [55] Sun YP, Zhou B, Lin Y, Wang W, Fernando KA, Pathak P, et al. Quantum-sized carbon dots for bright and colorful photoluminescence. | Am Chem Soc. 2006;128(24):7756-7.
- [56] Li XY, Wang HQ, Shimizu Y, Pyatenko A, Kawaguchi K, Koshizaki N. Preparation of carbon quantum dots with tunable

- photoluminescence by rapid laser passivation in ordinary organic solvents. Chem Commun. 2011;47(3):932-4.
- [57] Shang W, Cai T, Zhang Y, Liu D, Liu S. Facile one pot pyrolysis synthesis of carbon quantum dots and graphene oxide nanomaterials: All carbon hybrids as eco-environmental lubricants for low friction and remarkable wear-resistance. Tribol Int. 2018;118:373-80.
- Mehta VN, Jha S, Basu H, Singhal RK, Kailasa SK. One-step hydrothermal approach to fabricate carbon dots from apple juice for imaging of mycobacterium and fungal cells. Sens Actuators B: Chem. 2015;213:434-43.
- [59] Xue MY, Zhan ZH, Zou MB, Zhang LL, Zhao SL. Green synthesis of stable and biocompatible fluorescent carbon dots from peanut shells for multicolor living cell imaging. N J Chem. 2016:40(2):1698-703.
- [60] Soumen C, Ray CA, Dipranjan L, Kumar SS. Fabrication of nitrogen- and phosphorous-doped carbon dots by the pyrolysis method for iodide and iron(III) sensing. Lumin: J Biol Chem Lumi. 2018;33(2):336-44.
- [61] Supchocksoonthorn P, Hanchaina R, Sinoy MCA, de Luna MDG, Kangsamaksin T, Paoprasert P. Novel solution-and paper-based sensors based on label-free fluorescent carbon dots for the selective detection of pyrimethanil. Appl Surf Sci. 2021:564:150372.
- Zhu H, Wang XL, Li YL, Wang ZJ, Yang F, Yang XR. Microwave [62] synthesis of fluorescent carbon nanoparticles with electrochemiluminescence properties. Chem Commun. 2009;34:5118-20.
- [63] Qin X, Lu W, Asiri AM, Al-Youbi AO, Sun X. Microwave-assisted rapid green synthesis of photoluminescent carbon nanodots from flour and their applications for sensitive and selective detection of mercury(II) ions. Sens Actuators: B Chem. 2013;184:156-62.
- [64] Wei Y, Zhang D, Fang Y, Wang H, Liu Y, Xu Z, et al. Detection of ascorbic acid using green synthesized carbon quantum dots. I Sens. 2019;2019:1-10.
- [65] Zhang HQ, Wang H, Wang Y, Xin BF. Controlled synthesis and photocatalytic performance of biocompatible uniform carbon quantum dots with microwave absorption capacity. Appl Surf Sci. 2020;512:145751.
- Architha NRM, Shobana C. Microwave-assisted green synthesis of fluorescent carbon quantum dots from Mexican Mint extract for Fe<sup>3 +</sup> detection and bio-imaging applications. Environ Res. 2021:199:111263.
- [67] Lu Z, Su T, Feng Y, Jiang S, Zhou C, Hong P, et al. Potential application of nitrogen-doped carbon quantum dots synthesized by a solvothermal method for detecting silver ions in food packaging. Int J Environ Res Public Health. 2019;16(14):2518.
- [68] Xu XY, Yan B. Fabrication and application of a ratiometric and colorimetric fluorescent probe for Hg<sup>2+</sup> based on dual-emissive metal organic framework hybrids with carbon dots and Eu<sup>3+</sup>. J Mater Chem C. 2016;4(7):1543-9.
- [69] Bourlinos AB, Stassinopoulos A, Anglos D, Zboril R, Karakassides M, Giannelis EP. Surface functionalized carbogenic quantum dots. Small. 2008;4(4):455-8.
- [70] Xu JY, Zhou Y, Liu SX. Low-cost synthesis of carbon nanodots from natural products used as a fluorescent probe for the detection of ferrum(III) ions in lake water. Anal Methods. 2014;6(7):2086-90.
- [71] Huang YT, Liao WG. Hierarchical carbon material of N-doped carbon quantum dots in-situ formed on N-doped carbon nanotube for efficient oxygen reduction. Appl Surf Sci. 2019:495:143597.

- [72] Huang X, Bao R, Yi JH. Improving effect of carbonized quantum dots (CQDs) in pure copper matrix composites. J Cent South Univ. 2021;28(4):1255-65.
- [73] Molaei MJ. Principles, mechanisms, and application of carbon quantum dots in sensors: a review. Anal Methods. 2020;12(10):1266-87.
- [74] Akbarpour MR, Alipour S, Farvizi M, Kim HS. Mechanical, tribological and electrical properties of Cu-CNT composites fabricated by flake powder metallurgy method. Arch Civ Mech Eng. 2019;19(3):694-706.
- [75] Sheng M, Zhang G, Wang J, Yang Q, Zhao H, Cheng X, Xu Z. Preparation mechanism of hierarchical layered structure of graphene/copper composite with ultrahigh tensile strength. Carbon. 2018:127:329-39.
- [76] Xiong N, Bao R, Yi J, Fang D, Tao JM, Liu YC. CNTs/Cu-Ti composites fabrication through the synergistic reinforcement of CNTs and in situ generated nano-TiC particles. J Alloy Compd. 2019;770:204-13.
- [77] Berndt CC, Lavernia EJ. Thermal spray processing of nanoscale materials - A conference report with extended abstract. J Therm Spray Technol. 1998;7(3):411-40.
- [78] George R, Kashyap KT, Rahul R, Yamdagni S. Strengthening in carbon nanotube/aluminium (CNT/Al) composites. Scr Mater. 2005;53(10):1159-63.
- [79] Poirier D, Gauvin R, Drew RAL. Structural characterization of a mechanically milled carbon nanotube/aluminum mixture. Compos Part A. 2009;40(9):1482-89.
- [80] Singh SCE, Selvakumar N. Effect of milled B4C nanoparticles on tribological analysis, microstructure and mechanical properties of Cu-4Cr matrix produced by hot extrusion. Arch Civ Mech Eng. 2017;17(2):446-56.
- [81] Varo T, Canakci A. Effect of the CNT content on microstructure, physical and mechanical properties of Cu-based electrical contact materials produced by flake powder metallurgy. Arab J Sci Eng. 2015;40(9):2711-20.
- [82] Varol T, Canakci A. The effect of type and ratio of reinforcement on the synthesis and characterization Cu-based nanocomposites by flake powder metallurgy. J Alloy Compd. 2015;649:1066-74.
- [83] Akbarpour MR, Alipour S, Naiafi M, Tribological characteristics of self-lubricating nanostructured aluminum reinforced with multi-wall CNTs processed by flake powder metallurgy and hot pressing method. Diam & Relat Mater. 2018;90: 93-100.
- [84] Cha SI, Kim KT, Arshad SN, Mo CB, Hong SH. Extraordinary strengthening effect of carbon nanotubes in metal-matrix nanocomposites processed by molecular-level mixing. Adv Mater. 2005;17(11):1377-81.
- [85] Zhao C. Enhanced strength in reduced graphene oxide/nickel composites prepared by molecular-level mixing for structural applications. Appl Phys A. 2015;118(2):409-16.
- [86] Duraisamy S, Suppan T, Mohanta K. Novel synthesis of Cu<sub>2</sub>CoSnS<sub>4</sub>-carbon quantum dots nano-composites potential light absorber for hybrid photovoltaics. Nanotechnology. 2020;31(23):235401.
- [87] Xia QX, Yao ZP, Zhang DJ. Rational synthesis of micronano dendritic ZVI@ Fe<sub>3</sub>O<sub>4</sub> modified with carbon quantum dots and oxygen vacancies for accelerating Fenton-like oxidation. Sci Total Environ. 2019:671:1056-65.

- [88] Hwang J, Yoon T, Jin SH. Enhanced mechanical properties of graphene/copper nanocomposites using a molecular-level mixing process. Adv Mater. 2013;25(46):6724-9.
- [89] Kim KT, Eckert J, Liu G, Park JM, Lim BK, Hong SH. Influence of embedded-carbon nanotubes on the thermal properties of copper matrix nanocomposites processed by molecular-level mixing. Scr Mater. 2011;64(2):181-4.
- Dae PG, Chan KY. One-pot synthesis of CoSex -rGO composite powders by spray pyrolysis and their application as anode material for sodium-ion batteries. Chemistry. 2016;22(12):4140-6.
- [91] Yang S, Park GD, Kang YC. Conversion reaction mechanism of cobalt telluride-carbon composite microspheres synthesized by spray pyrolysis process for K-ion storage. Appl Surf Sci. 2020:529:147140.
- [92] Zhang L, Bao R, Yi J, Guo S, Tao J, Li C, et al. Improving comprehensive performance of copper matrix composite by spray pyrolysis fabricated CNT/W reinforcement. J Alloy Compd. 2020;833:154940.
- Taghian DS, Ali D, André M. Thermally sprayed metal matrix composite coatings as heating systems. Appl Therm Eng. 2021:196:117321.
- [94] Sharma V, Kaur M, Bhandari S. Micro and nano ceramic-metal composite coatings by thermal spray process to control slurry erosion in hydroturbine steel: an overview. Eng Res Express. 2019;1(1):012001.
- Cheng Z, Wei W, Cheng LY, Ge YY, Yue W, Lin L. 3D printing of Fe-[95] based bulk metallic glasses and composites with large dimensions and enhanced toughness by thermal spraying. J Mater Chem A. 2018;6(16):6800-5.
- Elugoke SE, Fayemi OE, Adekunle AS, Mamba BB, Nkambule TTI, [96] Ebenso EE. Electrochemical sensor for the detection of dopamine using carbon quantum dots/copper oxide nanocomposite modified electrode. FlatChem. 2022;33:100372.
- [97] Algarra M, González-Calabuig A, Radotić K, Mutavdzic D, Ania CO, Lázaro-Martínez JM, et al. Enhanced electrochemical response of carbon quantum dot modified electrodes. Talanta. 2018;178:679-85.
- Huang Q, Hu S, Zhang H, Chen J, He Y, Li F, et al. Carbon dots and chitosan composite film based biosensor for the sensitive and selective determination of dopamine. Analyst. 2013:138(18):5417-23.
- [99] Zhu HW, Liu Z, Cheng ZL. Stable dispersed N-doped carbon quantum dots-decorated 2D Ni-BDC nanocomposites towards the tribological application. Appl Surf Sci. 2022;582:152428.
- [100] Liu R, Huang H, Li H, Liu Y, Zhong J, Li Y, et al. Metal nanoparticle/ carbon quantum dot composite as a photocatalyst for high-efficiency cyclohexane oxidation. ACS Catal. 2014;4(1):328-36.
- [101] Wang WJ, Yung KC, Tang AD, Choy HS, lv Z. Evolution of microstructure, texture and mechanical properties for multilayered Al matrix composites by accumulative roll bonding. Materials. 2021;14(19):5576.
- [102] Chen B, Shen J, Ye X, Jia L, Li S, Umeda J, et al. Length effect of carbon nanotubes on the strengthening mechanisms in metal matrix composites. Acta Mater. 2017;140:317-25.
- [103] Tan J, Zou R, Zhang J, Li W, Zhang L, Yue D. Large-scale synthesis of N-doped carbon quantum dots and their phosphorescence properties in a polyurethane matrix. Nanoscale. 2016;8(8):4742-7.
- [104] Huang H, Hu H, Qiao S, Bai L, Han M, Liu Y, et al. Carbon guantum dot/CuS<sub>x</sub> nanocomposites towards highly efficient lubrication and metal wear repair. Nanoscale. 2015;7(26):11321-7.

- [105] Li S, Su W, Wu H, Yuan T, Yuan C, Liu J, et al. Carbon quantum dots enhanced the activity for the hydrogen evolution reaction in ruthenium-based electrocatalysts. Mater Chem Front. 2020;4(1):277-84.
- [106] Lin Q, Shen P, Yang L, Jin S, Jiang Q. Wetting of TiC by molten Al at 1123-1323K. Acta Mater. 2011;59:1898-911.
- [107] Nogi K, Hirata Y, Matsumoto T, Fujii H. Reactive wetting in liquid Cu alloy-carbon and silicon carbide systems. J Phys: Conf Ser. 2009:165(1):1-6.
- [108] Aksay IA, Hoge CE, Pask JA. Wetting under chemical equilibrium and nonequilibrium conditions. J Phys Chem. 1974;78(12):1178-83.
- [109] Voytovych R, Robaut F, Eustathopoulos N. The relation between wetting and interfacial chemistry in the CuAgTi/alumina system. Acta Mater. 2006;54(8):2205-14.
- [110] Mao W. Yamaki T. Miyoshi N. Shinozaki N. Ogawa T. Wettability of Cu-Ti alloys on graphite in different placement states of copper and titanium at 1373K (1100°C). Metall Mater Trans A. 2015;46:2262-72.
- [111] Mortimer DA, Nicholas M. The wetting of carbon and carbides by copper alloys. J Mater Sci. 1973;8(5):640-8.
- [112] Wan YZ, Wang YL, Luo HL, Dong XH, Cheng GX. Effects of fiber volume fraction, hot pressing parameters and alloying elements on tensile strength of carbon fiber reinforced coppe matrix composite prepared by continuous three-step electrodeposition. Mater Sci & Eng A. 2000;288(1):26-33.
- [113] Kishkoparov NV, Chentsov VP, Frishberg IV. Wetting of natural graphite by copper alloys. Powder Metall Met Ceram. 1984;23(11):869-70.
- Naidich YV, Kolesnichenko GA. A study of wetting of diamond and [114] graphite by fused metals and alloys VII. The effect of vanadium, niobium, manganese, molybdenum, and tungsten on wetting of graphite by copper-based alloys. Sov Powder Metall Met Ceram. 1968;7(7):563-5.
- [115] Yang LL, Shen P, Lin QL. Effect of Cr on the wetting in Cu/graphite system. Appl Surf Sci. 2011;257:6276-81.
- [116] Zhang H, Xiong J, Guo ZX, Yang TE, Liu JB, Hua T. Microstructure, mechanical properties, and cutting performances of WC-Co cemented carbides with Ru additions. Ceram Int. 2021:47(18):26050-62.
- Yang W, Zhou L, Peng K. Effect of tungsten addition on thermal [117] conductivity of graphite/copper composites. Composites Part B: Engineering. 2013;55:1-4.
- [118] Lim SY, Shen W, Gao ZQ. Carbon quantum dots and their applications. Chem Soc Rev. 2015;44(1):362-81.
- Tian L, Li Z, Wang P, Zhai XH, Wang X, Li TX. Carbon quantum dots for advanced electrocatalysis. J Energy Chem. 2021;55:279-94.
- [120] Das R, Bandyopadhyay R, Pramanik P. Carbon quantum dots from natural resource: A review. Mater Today Chem. 2018;8:96-109.
- [121] Sayyad R, Ghambari M, Ebadzadeh T, Pakseresht AH. Preparation of Ag/reduced graphene oxide reinforced copper matrix composites through spark plasma sintering: an investigation of microstructure and mechanical properties. Ceram Int. 2020;46(9):13569-79.
- Ye M, Cai T, Shang W. Friction-induced transfer of carbon [122] quantum dots on the interface: Microscopic and spectroscopic studies on the role of inorganic-organic hybrid nanoparticles as multifunctional additive for enhanced lubrication. Tribol Int. 2018:127:557-67.
- [123] Kong J, Zhang C, Cheng X. Novel Cu-Cr alloy matrix CNT composites with enhanced thermal conductivity. Appl Phys A. 2013;112:631-6.

- [124] Cho S, Kikuchi K, Miyazaki T. Multiwalled carbon nanotubes as a contributing reinforcement phase for the improvement of thermal conductivity in copper matrix composites. Scr Mater. 2010;63(4):375–8.
- [125] Bandi R, Gangapuram BR, Dadigala R, Eslavath R, Singh SS, Guttena V. Facile and green synthesis of fluorescent carbon dots from onion waste and their potential applications as sensor and multicolour imaging agents. RSC Adv. 2016;6(34):28633–9.
- [126] He Z, Liang R, Zhou C, Yan G, Wu L. Carbon quantum dots (CQDs)/ noble metal co-decorated MIL-53(Fe) as difunctional photocatalysts for the simultaneous removal of Cr(VI) and dyes. Sep Purif Technol. 2021;255:117725.
- [127] Fan L, Wang Y, Li L. Carbon quantum dots activated metal organic frameworks for selective detection of Cu (II) and Fe (III). Colloids Surf A: Physicochem Eng Asp. 2020;588:124378.
- [128] Zhao S, Li C, Wang L, Liu N, Qiao S, Liu B, et al. Carbon quantum dots modified MoS<sub>2</sub> with visible-light-induced high hydrogen evolution catalytic ability. Carbon. 2016;99:599–606.
- [129] Zou PG, Hou H, Hu PJ, Ji PX. General synthesis of heteroatom-doped hierarchical carbon toward excellent electrochemical energy storage. Batteries Supercaps. 2019;2(8):712–22.
- [130] Kou XL, Jiang SC, Park SJ, Meng LY. A review: recent advances in preparations and applications of heteroatom-doped carbon quantum dots. Dalton Trans. 2020;49(21):6915–38.
- [131] Wang X, Feng YQ, Dong PP. A mini review on carbon quantum dots: preparation, properties, and electrocatalytic application. Front Chem. 2019;7:671.
- [132] Kannan R, Jang HR, Yoo ES. Facile green synthesis of palladium quantum dots@ carbon on mixed valence cerium oxide/graphene hybrid nanostructured bifunctional catalyst for electrocatalysis of alcohol and water. RSC Adv. 2015;5(45):35993–6000.
- [133] Cheng H, Li ML, Su CY, Cu C. Bimetallic oxide quantum dot decorated nitrogen-doped carbon nanotubes: a high-efficiency bifunctional oxygen electrode for Zn-air batteries. Adv Funct Mater. 2017;27:1701833.
- [134] Dave K, Gomes VG. Carbon quantum dot-based composites for energy storage and electrocatalysis: mechanism, applications and future prospects. Nano Energy. 2019;66:104093.
- [135] Han G, Zhao J, Zhang R, Tian X, Liu Z, Wang A, et al. Carbon quantum dots modulated NiMoP hollow nanopetals as efficient electrocatalysts for hydrogen evolution. Ind Eng Chem Res. 2019;58(31):14098–105.
- [136] Zhang LJ, Yang YM, Ziaee MA, Lu KL, Wang RH. Nanohybrid of carbon quantum dots/molybdenum phosphide nanoparticle for efficient electrochemical hydrogen evolution in alkaline medium. ACS Appl Mater Interfaces. 2018;10(11):9460–7.
- [137] Raikwar VR. Synthesis and study of carbon quantum dots (CQDs) for enhancement of luminescence intensity of CQD@LaPO<sub>4</sub>: Eu<sup>3+</sup>nanocomposite. Mater Chem Phys. 2022;275:125277.
- [138] Jing M, Wang J, Hou H, Yang Y, Zhang Y, Pan C, et al. Carbon quantum dot coated Mn3O4 with enhanced performances for lithium-ion batteries. J Mater Chem A. 2015;3(32):16824–30.
- [139] Navidfar A, Peker MI, Budak E, Unlu C, Trabzon L. Carbon quantum dots enhanced graphene/carbon nanotubes polyurethane hybrid nanocomposites. Compos Part B: Eng. 2022:247:110310.
- [140] Latif Z, Shahid K, Anwer H, Shahid R, Ali M, Lee KH, Alshareef M. Carbon quantum dots (CQDs)-modified polymers: a review of non-optical applications. Nanoscale. 2024;16:2265–88.

- [141] Dager A, Uchida T, Maekawa T, Tachibana M. Synthesis and characterization of mono-disperse carbon quantum dots from fennel seeds: photoluminescence analysis using machine learning. Sci Rep. 2019;9(1):14004.
- [142] Lin SY, Shen W, Gao ZQ. Carbon quantum dots and their applications. Chem Soc Rev. 2015;44(1):362–81.
- [143] Zaheri M, Aklima N, Mahbub H, Gomes VG. 3D-printed polymer nanocomposites with carbon quantum dots for enhanced properties and in situ monitoring of cardiovascular stents. Polym Adv Technol. 2022;33(3):980–90.
- [144] Tong W, Fang D, Bao C, Tan S, Liu Y, Li F, et al. Enhancing mechanical properties of copper matrix composite by adding SiO2 quantum dots reinforcement. Vacuum. 2022;195:110682.
- [145] Kelly A, Tyson WR. Tensile properties of fibre-reinforced metals: Copper/tungsten and copper/molybdenum. J Mech Phys Solids. 1965;13(6):329–50.
- [146] Yu BY, Kwak SY. Carbon quantum dots embedded with mesoporous hematite nanospheres as efficient visible light-active photocatalysts. J Mater Chem. 2012;22(17):8345–53.
- [147] Elomari S, Boukhili R, Lloyd DJ. Thermal expansion studies of prestrained Al<sub>2</sub>O<sub>3</sub>/Al metal matrix composite. Acta Mater. 1996;44(5):1873–82.
- [148] Nie JF, Barrington CM. Strengthening of an Al–Cu–Sn alloy by deformation-resistant precipitate plates. Acta Mater. 2008;56(14):3490–501.
- [149] Zhang Z, Chen DL. Consideration of Orowan strengthening effect in particulate-reinforced metal matrix nanocomposites: A model for predicting their yield strength. Scr Mater. 2006;54(7):1321–6.
- [150] Wen Y, Zhu G, Shao Y. Improving the power conversion efficiency of perovskite solar cells by adding carbon quantum dots. J Mater Sci. 2020;55(7):2937–46.
- [151] Guan J, Song M, Chen L, Shu Y, Jin D, Fan G, et al. Carbon quantum dots passivated CsPbBr<sub>3</sub> film with improved water stability and photocurrent: Preparation, characterization and application. Carbon. 2021;175:93–100.
- [152] Liu D, Ding Y, Guo T, Qin X, Guo C, Yu S, Lin S. Influence of fine-grain and solid-solution strengthening on mechanical properties and in vitro degradation of WE43 alloy. Biomed Mater. 2014;9(1):015014.
- [153] Bao T, Song L, Zhang S. Synthesis of carbon quantum dot-doped NiCoP and enhanced electrocatalytic hydrogen evolution ability and mechanism. Chem Eng J. 2018;351:189–94.
- [154] He JQ, Sun JL, Choi J, Wang CL, Su DX. Synthesis of N-doped carbon quantum dots as lubricant additive to enhance the tribological behavior of MoS<sub>2</sub> nanofluid. Friction. 2023;11(3):441–59.
- [155] Yin YZ, Lu HH, Song WJ. Carbon quantum dot (CQD)-based composite fluorescent hydrogel for the isolation and determination of iron (III). Anal Lett. 2023;2262631.
- [156] Hou HS, Banks CE, Jing MJ, Zhang Y, Ji XB. Sodium-ion batteries: carbon quantum dots and their derivative 3D porous carbon frameworks for sodium-ion batteries with ultralong cycle life. Adv Mater. 2015;27(47):7861–6.
- [157] Zhu Y, Ji X, Pan C, Sun Q, Song W, Fang L, et al. A carbon quantum dot decorated  $RuO_2$  network:outstanding supercapacitances under ultrafast charge and discharge. Energy Environ Sci: EES. 2013;6(12):3665–75.
- [158] Liu F, Wang Y, Zhang Y, Lin J, Su Q, Shi J, et al. A facile carbon quantum dot-modified reduction approach towards tunable Sb@CQDs nanoparticles for high performance sodium storage. Batteries Supercaps. 2020;3(5):463–9.

- [159] Zhang PY, Zeng GC, Song T, Huang SB, Wang TT, Zeng HP. Synthesis of a plasmonic CuNi bimetal modified with carbon quantum dots as a non-semiconductor-driven photocatalyst for effective water splitting. J Catal. 2019;369:267–75.
- [160] Zhao S, Li C, Liu J, Liu N, Qiao S, Han Y, et al. Carbon quantum dots/SnO<sub>2</sub>-Co<sub>3</sub>O<sub>4</sub> composite for highly efficient electrochemical water oxidation. Carbon. 2015;92:64–73.
- [161] Yang MX, Feng TL, Chen YX, Liu JJ, Zhao XH, Yang B. Synchronously integration of Co, Fe dual-metal doping in Ru@C and CDs for boosted water splitting performances in alkaline media. Appl Catal B: Environ. 2020;267:118657.
- [162] Tang D, Liu J, Wu XY, Liu RH, Han X, Han YZ. Carbon quantum dot/ NiFe layered double-hydroxide composite as a highly efficient electrocatalyst for water oxidation. ACS Appl Mater interfaces. 2014:6(10):7918–25.
- [163] Han G, Cai J, Liu C, Ren J, Wang X, Yang J, et al. Highly sensitive electrochemical sensor based on xylan-based Ag@CQDs-rGO nanocomposite for dopamine detection. Appl Surf Sci. 2021;541:148566.
- [164] Lin HQT, Lin XF, Zhang CQ, Hu Y, Wei SR. C. A high performance electrochemical biosensor based on Cu2O-carbon dots for selective and sensitive determination of dopamine in human serum. RSC Adv. 2015;5(67):54102–8.
- [165] Chen YW, Jiang YF, Chen BY, Ye FL, Duan HQ, Cui HY. Facile fabrication of N-doped carbon quantum dots modified SnO<sub>2</sub> composites for improved visible light photocatalytic activity. Vacuum. 2021;191:110371–138.
- [166] Tamal S, Tarun KD, Reena KS, Smriti S, Pratima RS. Studies on carbon-quantum-dot-embedded iron oxide nanoparticles and their electrochemical response. Nanotechnology. 2020;31(35):355502.
- [167] Martins NCT, Ângelo J, Girão AV, Trindade T, Andrade L, Mendes A. N-doped carbon quantum dots/TiO<sub>2</sub> composite with improved photocatalytic activity. Appl Catal B: Environ. 2016;193:67–74.
- [168] Zhu ZJ, Cheng R, Ling LT, Li Q, Chen S. Rapid and large-scale production of multi-fluorescence carbon dots by a magnetic hyperthermia method. Angew Chem (Int Ed). 2020;59(8):3099–105.
- [169] Anwar S, Ding H, Xu M, Hu X, Li Z, Wang J, et al. Recent advances in synthesis, optical properties, and biomedical applications of carbon dots. ACS Appl Bio Mater. 2019;2(6):2317–38.
- [170] Mancini F, Menichetti A, Degli Esposti L, Montesi M, Panseri S, Bassi G, et al. Fluorescent carbon dots from food industry byproducts for cell imaging. J Funct Biomater. 2023;14(2):90.

- [171] Deepika D, Kumar L, Gaikwad KK. Carbon dots for food packaging applications. Sustainable Food Technol. 2023;1(2):185–99.
- [172] Franco CA, Candela CH, Gallego J, Marin J, Patiño LE, Ospina N, et al. Easy and rapid synthesis of carbon quantum dots from Mortiño (Vaccinium Meridionale Swartz) extract for use as green tracers in the oil and gas industry: Lab-to-field trial development in Colombia. Ind Eng Chem Res. 2020:59(25):11359–69.
- [173] Palanimuthu K, Subbiah U, Sundharam S, Munusamy C. Spirulina carbon dots: a promising biomaterial for photocatalytic textile industry Reactive Red M8B dye degradation. Environ Sci Pollut Res Int. 2023;30(18):52073–86.
- [174] Berdimurodov E, Verma DK, Kholikov A, Akbarov K, Guo L. The recent development of carbon dots as powerful green corrosion inhibitors: A prospective review. J Mol Liq. 2022;349:118124.
- [175] Urushihara N, Hirai T, Dager A, Nakamura Y, Nishi Y, Inoue K, et al. Blue–green electroluminescent carbon dots derived from fenugreek seeds for display and lighting applications. ACS Appl Nano Mater. 2021;4(11):12472–80.
- [176] Cho S, Kikuchi K, Kawasaki A, Kwon H, Kim Y. Effective load transfer by a chromium carbide nanostructure in a multi-walled carbon nanotube/copper matrix composite. Nanotechnology. 2012;23(31):315705.
- [177] Veillère A, Sundaramurthy A, Heintz JM, Douin J, Lahaye M, Chandra N, et al. Relationship between interphase chemistry and mechanical properties at the scale of micron in Cu–Cr/CF composite. Acta Mater. 2011;59(4):1445–55.
- [178] Chu K, Jia CC, Li WS, Wang P. Mechanical and electrical properties of carbon-nanotube-reinforced Cu–Ti alloy matrix composites. Phys Status Solidi (a). 2013;210(3):594–9.
- [179] Tuccitto N, Fichera L, Ruffino R, Cantaro V, Sfuncia G, Nicotra G, et al. Carbon quantum dots as fluorescence nanochemosensors for selective detection of amino acids. ACS Appl Nano Mater. 2021:4(6):6250–6
- [180] Sakshi T, Pawan KS, Arun KT, Pritam P. Optimization and comparison of photovoltaic parameters of Zinc Oxide (ZnO)/ Graphene Oxide (GO) and Zinc Oxide (ZnO)/Carbon Quantum Dots (CQDs) hybrid solar cell using firefly algorithm for application in solar trigeneration system in commercial buildings. Sustainable Energy Technol Assess. 2021;47:101357.
- [181] Mirsaeidi AM, Yousefi F. Viscosity, thermal conductivity and density of carbon quantum dots nanofluids: an experimental investigation and development of new correlation function and ANN modeling. J Therm Anal Calorim. 2021;143:351–61.